THE SCHRÖDINGER EQUATION TO SPECTROSCOPY: A SIMPLIFIED QUANTUM MECHANICAL CONNECTION

_____

A Thesis

Presented to

The Faculty of the Department of Chemistry

Sam Houston State University

_____

In Partial Fulfillment

of the Requirements for the Degree of

Master of Science

_____

by

Victoria A Spenn

December, 2015

THE SCHRÖDINGER EQUATION TO SPECTROSCOPY: A SIMPLIFIED QUANTUM MECHANICAL CONNECTION

by

Victoria A Spenn

_____

APPROVED:

Dr. Darren L. Williams
Thesis Director

Dr. Benny E. Arney
Committee Member

Dr. David E. Thompson
Committee Member

Dr. John B. Pascarella, Dean
College of Sciences

DEDICATION

Click here to enter text. This section is optional. If you do not wish to compose a dedication, then delete this page using the navigation pane. If you are not sure whether you will compose a dedication, then you may refrain from deleting this page until you are sure.

ABSTRACT

Spenn, Victoria A, *The Schrödinger equation to spectroscopy: a simplified quantum mechanical connection*. Master of Science (Chemistry), December, 2015, Sam Houston State University, Huntsville, Texas.

Quantum mechanics was initially developed to answer contradictions between classical theory and experimental observations by providing a mathematical solution for the interaction of energy and matter. In order to make quantum mechanics more approachable, simple models like particle in a box and particle on a ring are used to explain energy quantization and wave function movement. This thesis expands on these classical systems. The expansion connects the Schrödinger equation to the transition dipole moment integral to create an absorbance spectrum or to the transition moment integral to create a Raman spectrum. The analytical approach provides an explicit calculus based solution while the numerical method exposes a dynamic view of electronic behavior, and the symmetry solution gives an easy construction of selection rules. All techniques lend to a better understanding and visualization of electronic behavior and a comprehension of spectroscopy at the quantum level.

KEY WORDS: Particle in a Box, Particle on a Ring, Spectroscopy, Raman Spectroscopy, Quantum Chemistry, Schrödinger Equation

ACKNOWLEDGEMENTS

Click here to enter text. This page is optional.

TABLE OF CONTENTS

Page

LIST OF FIGURES

FIGURE **Page**

LIST OF TABLES

CHAPTER I

Introduction

In an effort to make quantum mechanics more accessible, this thesis strives to link the basic particle in a box and particle on a ring systems to their corresponding spectral outputs. This will help explain the foundational concepts and ramifications of quantum mechanics. Currently these systems are used in physical chemistry books to show quantization of energy by solving the Schrödinger equation, and the behavior of the wave function as a function of changing quantum numbers and system size.

Present textbooks surprisingly do not connect the Schrödinger equation to the transition dipole moment integral as an explanation for widely emphasized failures of classical physics such as line spectra observation and phenomena from Planck, Einstein and Schrödinger. Specifically the Engel & Reid Physical Chemistry textbook and Atkins & de Paula Physical Chemistry textbook do inform the reader of the connection between selection rules and the transition dipole moment integral but do not give a detailed explanation as to what causes these selection rules or what can alter the output of this approximation. The idea of symmetry solving this integrand is touched upon, but it is not explained. There is also no connected between transition wavelengths produced from the Schrödinger equation and the intensity of these transitions.

Other scholars have expanded upon the particle in a box and the particle on a ring systems to explore and explain quantum mechanical ideas. Some have studied three particles in a one-dimensional box, and used group theory to describe the symmetry of the system.[1] Further expansion on the particle in a box include considering the wave function boundary conditions in connection to the uncertainty for a quantum dot with

perfectly reflecting walls.[2] The particle in a box problem has also been solved with a moving wall.[3] Quantum Zeno dynamics which shows the evolution of a quantum system undergoing frequent measurements has also been analyzed by applying particle in a box principles.[4]

New models have proposed a different confinement for a particle in a two-dimensional ring.[5] The particle on ring model has been used to derive alternative energy levels specifically for cyclic pi-systems.[6] Also, due to the high mathematical difficulty there have been many who try to simplify basic selection rules.[7–9]

Dirac Notation

In order to simplify the integral expressions, Dirac bracket notation will be implemented. For the following integral, the $|n>$ is the ket and represents the function f_n (eq 1).[10] The $<m|$ is the bra and represents the complex conjugate function f_{m*} (eq 1).[10] The bra and ket are also used with an operator such as Ω (eq 2).

$$\langle m|n\rangle = \int f_m^* f_n dx \quad (1)$$

$$\langle m|\Omega|n\rangle = \int f_m^* \Omega f_n dx \quad (2)$$

Particle in a Box

The particle in a box system is equivalent to a single particle, in this case an electron, moving freely in a box with impenetrable walls.[11] It will therefore mimic the electronic movement and spectroscopic possibilities of an electron. For the particle in a box system, a particle is confined in a box of a length *L*, with infinitely tall walls (*Figure 1*). Inside these walls the potential energy, *V*, is zero. The particle is freely moving, but outside the walls potential energy is infinite therefore giving the particle boundaries. The

simplicity of the system makes it possible to explain difficult mathematical quantum concepts in a one-dimensional case.

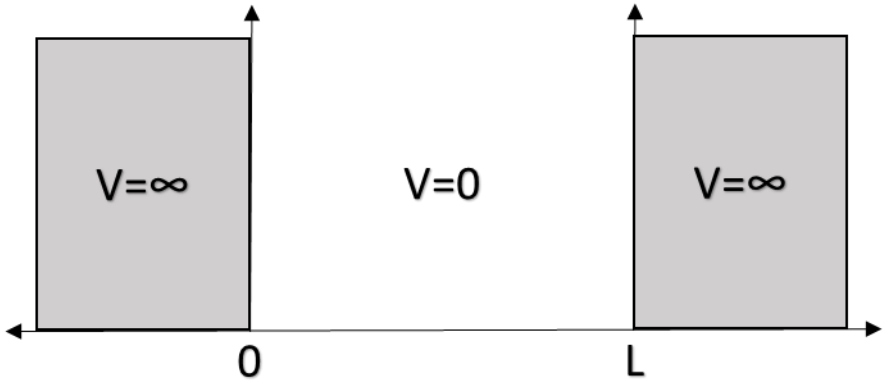

Figure 1. Particle in a box system.

Particle on a Ring

The particle on a ring system expresses the movement of an electron in a circular path and therefore will mimic the rotational movement and spectroscopic possibilities of an electron. In the particle on a ring system, a particle is constrained to move in a circle around the ring with radius *r* (*Figure 2*). With this system, as the particle is confined to move on a ring, potential energy is zero at all angles.

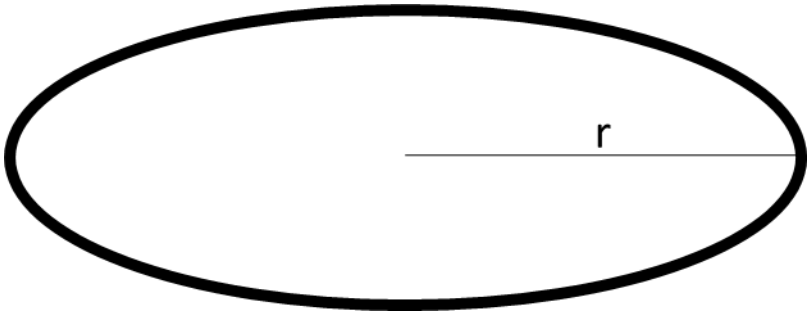

Figure 2. Particle on a ring system.

Wave function formulation

The movement of quantum particles will be described as wave functions. For each system, the particle will follow specific rules which constrains the wave function. For a particle in a box, the particle is bound inside the box by the potential energy difference and the wave functions must be continuous inside the box. Therefore, the wave functions are zero at the walls where $\psi(0)=0$ and $\psi(L)=0$.[11] These boundary conditions can be applied to the general wave function equation (eq 3). First, $\psi(0)=0$ is applied to give the general equation (eq 4). Since $\cos(0)=1$ and $\sin(0)=0$, the only way to satisfy the $\psi(0)=0$ condition is to set C=0 removing the cosine part of the general wave function. Next, $\psi(L)=0$ is applied to the general equation without the cosine function (eq 5). If *D* is set to zero the condition would be met but the wave function would always be zero making the particle not exist. Alternatively, *k* can be set to a constant that will give a multiple of π, in turn making sine go to zero and satisfying the boundary condition where *n* is the quantum number (eq 6).

$$\psi(x) = \mathrm{C}\cos(kx) + \mathrm{D}\sin(kx) \quad (3)$$

$$\psi(0) = \mathrm{C}\cos(0) + \mathrm{D}\sin(0) \quad (4)$$

$$\psi(L) = \mathrm{D}\sin(kL) \quad (5)$$

$$\psi(L) = \mathrm{D}\sin\left[\left(\frac{n\pi}{L}\right)L\right] \quad (6)$$

In the final particle in a box wave function, the quantum number is *n*, *L* is the length of the box, and *x* is the distance along the box length (eq 7).[11] This thesis will use a shifted wave function (eq 8). This shift is achieved by adding $n\pi/2$ to the argument within the sine function. Now instead of the box starting at 0 and going to *L*, it will start at $-L/2$

and go to *L/2*. The shift will allow *x*=0 to be used as the center of symmetry for the system.

$$\psi(x) = \sin\left(\frac{n\pi x}{L}\right) \quad (7)$$

$$\psi(x) = \sin\left(\frac{n\pi x}{L} + \frac{n\pi}{2}\right) \quad (8)$$

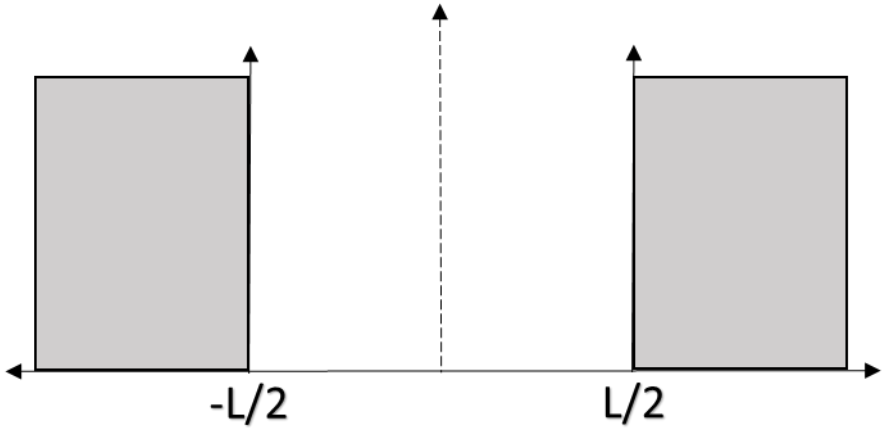

Figure 3. Shifted particle in a box system.

For the particle on a ring m_ℓ is defined as the rotational quantum number and ϕ as the rotational angle on the ring in radians (*Figure 4*). The wave function must be single valued and continuous around the ring so that ψ(0)=ψ(2π).[10] This condition is applied to the general wave function form (eq 9-10). Euler's relation can expand these wave functions and prove that this condition is met (eq 11). Both sine functions will go to zero as any π multiple will give a zero output. The cosine functions are both equal since the cosine of a 2π multiple and the cosine of zero are both equal to one. The condition of equation 10 is met as long as m_ℓ is any positive or negative integer or zero.

$$\psi(\phi) = Ae^{im_\ell\phi} \quad (9)$$

$$Ae^{i2\pi m_\ell} = Ae^{i0m_\ell} \quad (10)$$

$$\cos(2\pi m_\ell) + i\sin(2\pi m_\ell) = \cos(0m_\ell) + i\sin(0m_\ell) \qquad (11)$$

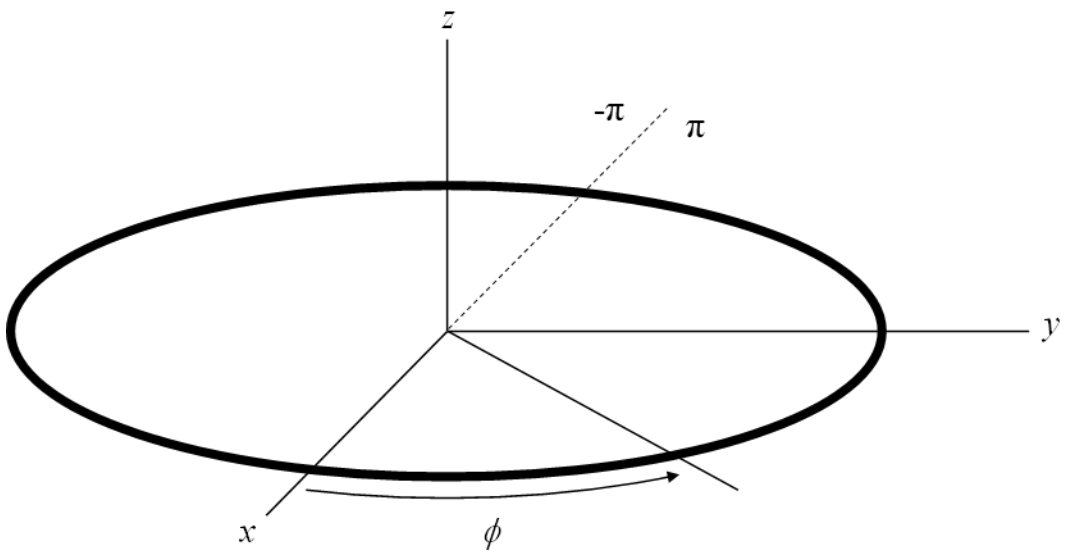

Figure 4. One dimensional ring with defined coordinate system and rotational angle.

Using Euler's relation, the final particle on a ring wave function can be expanded to equation 13 to separate the real and imaginary portions of the wave function.[10] Both negative and positive integers can be used as quantum numbers showing a degeneracy for $m_\ell \neq 0$, this is interpreted as forward and backward rotation (*Figure 5*). A shift in this equation is achieved by merely starting the wave function at $\phi=\pi$ and continuing to $\phi=-\pi$. This puts the center of symmetry at $\phi = 0$.

$$\psi(\phi) = e^{im_\ell\phi} \qquad (12)$$

$$\psi(\phi) = (\cos m_\ell\phi + i\sin m_\ell\phi) \qquad (13)$$

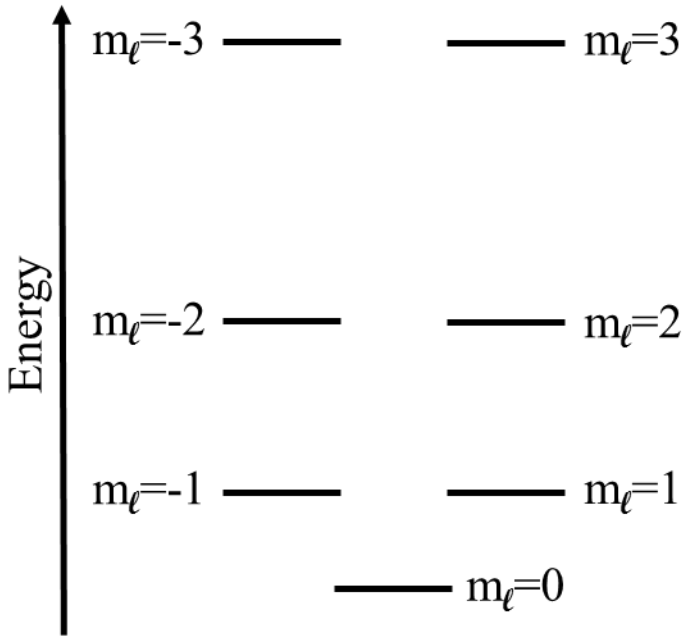

Figure 5. Particle on a ring energy diagram.

The Schrödinger equation

The Schrödinger equation is used to calculate the energy, *E*, of the wave function at each quantum level.[11] In the use of the particle in a box and particle on a ring systems, the interest is only in the spatial dependence of the wave function, so the following time-independent Schrödinger equation is used (eq 14).[10] The Hamiltonian operator $\hat{H}$ is a second derivative operator which returns the original wave function while extracting curvature information about the associated wave function, ψ (eq 14).[10] This is an eigenvalue equation, and the constant, energy, is the eigenvalue.

$$\hat{H}\psi = E\psi \qquad (14)$$

To solve the Schrödinger equation, the Hamiltonian operator for each system must be defined. The Hamiltonian is the operator for the total energy of a system (eq 15). For the particle in a box system, the free moving particle is confined within a box where

in the potential energy is zero (eq 16).[10] Since the potential energy is zero, the potential energy operator *V(x)* may be removed. In this Hamiltonian, $\hbar$ is Planck's constant divided by 2π (eq 17), and *m* is the mass of the particle.[10]

$$\hat{\mathrm{H}} = -\frac{\hbar^2}{2m}\frac{d^2}{dx^2} + V(x) \tag{15}$$

$$V(x) = \begin{cases} 0 & for\ 0 \le x \le L \\ \infty & otherwise \end{cases} \tag{16}$$

$$\hbar = \frac{h}{2\pi} \tag{17}$$

The particle on a ring models a particle travelling in the xy-plane in a circle at some radius *r*. Since the particle moves within the xy-plane, this system's Hamiltonian must take into account both the x and y coordinates (eq 18). By converting to polar coordinates, a simplified Hamiltonian is obtained where ϕ is the rotational angle ranging from 0 to 2π (eq 19).[10] In a rotating system, the moment of inertia, mr^2, takes the place of mass in the Hamiltonian.

$$\hat{\mathrm{H}} = -\frac{\hbar^2}{2m}\left(\frac{d^2}{dx^2} + \frac{d^2}{dy^2}\right) \tag{18}$$

$$\hat{\mathrm{H}} = -\frac{\hbar^2}{2mr^2}\left(\frac{d^2}{d\phi^2}\right) \tag{19}$$

Transition Dipole Moment Integral

The intensity of a transition is proportional to the square of the transition dipole moment integral.[10] The integral includes the initial wave function, ψ_i, the final excited wave function, ψ_f, and the electric dipole operator, μ_x, normally associated with light (eq 20).

$$I \propto \langle \psi_i | \mu_x | \psi_f \rangle^2 \tag{20}$$

If only evaluating the zero versus non-zero nature of the transition dipole moment integral, the selection rules for spectroscopic transitions can be determined. These determine which transitions one would expect to see in the spectrum, but they do not distinguish the intensity at which these transitions will be seen.[12] If the integral value is a non-zero, the transition is allowed, and if the integral value is zero, the transition is forbidden.[12] These allowed and forbidden transitions will form a trend that generate the selection rules.

Transition Moment Integral

With these models, Rayleigh and Raman scattering can also be observed with the same type of approximation. This can be done by using the polarizability operator (α) in the transition moment integral (eq 21).

$$I \propto \langle \psi_i | \, \hat{\alpha} \, | \psi_f \rangle^2 \qquad (21)$$

A Raman spectrum shows inelastic scattering of a photon. This happens when a molecule absorbs a photon which loses or gains some energy from the molecule and then leaves the molecule with a different energy.[10] Compared to the incidental light, Stokes will scatter a particle of lower energy and anti-Stokes will scatter a particle of higher energy (*Figure 6*). Alternatively, Rayleigh scattering is elastic scattering where the energy of a particle is the same going in as it is going out.[10]

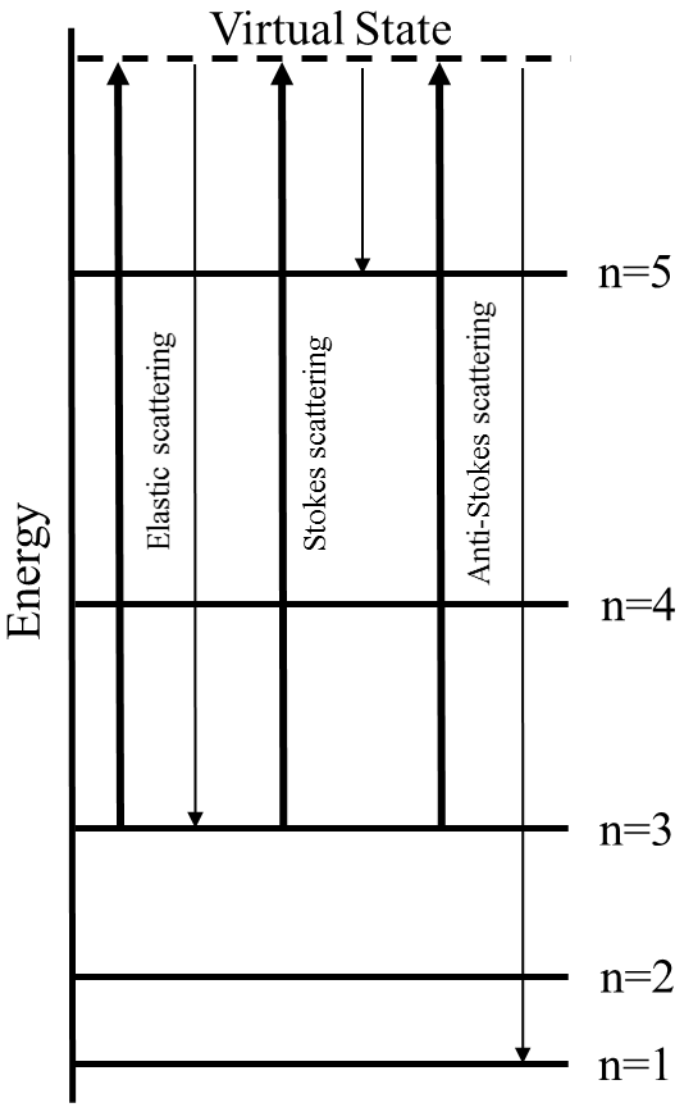

Figure 6. Elastic and inelastic scattering on an energy diagram system.

Though many other expansions upon these classical systems exist, none have modeled electronic excitation and the resulting spectrum. By using simple systems like the particle in a box and the particle on a ring, the mathematics can be simplified in a way to show the basic reasoning behind spectroscopic measurements. This project intends to produce a teaching tool connecting the Schrodinger equation with the transition dipole moment and transition moment integral in order to generate a theoretical spectrum and

determine selection rules. Generated are the normalized constants, the energy levels, the spectral lines and relative spectral intensities for direct absorption/emission, Raman scattering and Rayleigh scattering. This thesis provides analytical, numerical and symmetry-based solutions to the particle in a box and particle on a ring giving a variety of pedagogical possibilities.

CHAPTER II

Analytical Theory

The analytical theory is the calculus based computation, which gives an exact solution. Resulting from the Schrödinger equation, the particle in a box and particle on a ring expresses a particle's movement as a wave function in a one dimensional box or ring providing a visualization of quantum mechanics in a simplified system.[11]

Orthonormality

First, the wave functions must satisfy the orthonormality conditions in which the wave functions are normalized and mutually orthogonal.[10] The Kronecker delta (δ_{mn}) expresses this condition being equal to 1 when $m=n$ and equal to 0 when $m\neq n$ (eq 22).[10]

$$\langle n|m\rangle = \delta_{mn} \qquad (22)$$

For a quantum system, the probability distribution is determined by the square of the wave function of the current state.[11] Since the particle must be found somewhere in the box or ring, the integral of the probability distribution over all space should equal 1 (eq 23.1 & 24.1).[11] This restriction is met by having a normalization constant, *N*, included in the wave function. Equations 23.1-23.3 show the result of integration of the sine squared function for the particle in a box. The full set of steps is shown in Appendix A. Solving the first part of the integrand will give the normalization constant while the second part equals zero because all sine arguments are integer multiples of π (eq 23.3). Equation 23.4 shows the final normalized wave function.

$$\int_{-L/2}^{L/2} \left[N \sin\left(\frac{n\pi x}{L} + \frac{n\pi}{2}\right)\right]^2 dx = 1 \qquad (23.1)$$

$$\frac{N^2}{2} x \Big|_{-\frac{L}{2}}^{\frac{L}{2}} - \frac{N^2}{2} * \frac{L}{2n\pi} \sin\left(\frac{2n\pi x}{L} + n\pi\right) \Big|_{-\frac{L}{2}}^{\frac{L}{2}} = 1 \qquad (23.2)$$

$$N = \sqrt{\frac{2}{L}} \tag{23.3}$$

$$\psi(x) = \sqrt{\frac{2}{L}} \sin\left(\frac{n\pi x}{L} + \frac{n\pi}{2}\right) \tag{23.4}$$

Since the particle on a ring has an imaginary portion, the probability distribution equation shows the wave function multiplied by its complex conjugate (eq 24.1). After the integral is calculated, the normalization constant is determined (eq 24.2-24.3) Equation 24.4 shows the final normalized wave function for a particle on a ring.

$$\int_{-\pi}^{\pi} Ne^{-im_\ell \phi} * Ne^{im_\ell \phi} d\phi = 1 \tag{24.1}$$

$$N^2 \phi|_{-\pi}^{\pi} = 1 \tag{24.2}$$

$$N = \sqrt{\frac{1}{2\pi}} \tag{24.3}$$

$$\psi(\phi) = \sqrt{\frac{1}{2\pi}} e^{im_\ell \phi} \tag{24.4}$$

The wave functions must also be determined as orthogonal which means the wave functions in different quantum states are linearly independent.[10] This is determined by computing the overlap integral which is the integral of two different wave functions multiplied by each other, over all space (eq 25.1&26.1). Equation 25.3 shows the evaluation step for particle in a box. Since sine of 0 and any multiple of π is equal to zero, both arguments go to zero. The full set of these steps are shown in Appendix B.

$$\langle n|n'\rangle = 0 \; where \; n \neq n' \tag{25.1}$$

$$\int_{-L/2}^{L/2} \sqrt{\frac{2}{L}} \sin\left(\frac{n\pi x}{L} + \frac{n\pi}{2}\right) * \sqrt{\frac{2}{L}} \sin\left(\frac{n\prime\pi x}{L} + \frac{n\prime\pi}{2}\right) dx \tag{25.2}$$

$$\frac{1}{n\pi - n'\pi} \sin\left(\frac{n\pi x - n\prime\pi x}{L} + \frac{n\pi - n\prime\pi}{2}\right)\Big|_{-\frac{L}{2}}^{\frac{L}{2}} - \frac{1}{n\pi + n'\pi} \sin\left(\frac{n\pi x + n\prime\pi x}{L} + \frac{n\pi + n\prime\pi}{2}\right)\Big|_{-\frac{L}{2}}^{\frac{L}{2}} = 0 \tag{25.3}$$

Equation 26.3 shows the evaluation for particle on a ring. The log base e function in both arguments will equal -1. Therefore, each argument will cancel out and the integral will equal 0 and prove the orthogonality of this wave function.

$$\langle m_\ell | m'_\ell \rangle = 0 \tag{26.1}$$

$$\int_{-\pi}^{\pi} \sqrt{\frac{1}{2\pi}} e^{-im_\ell \phi} \sqrt{\frac{1}{2\pi}} e^{im'_\ell \phi} d\phi \tag{26.2}$$

$$\frac{1}{2\pi} \frac{1}{i(-m'_\ell + m_\ell)} e^{i\phi(-m'_\ell + m_\ell)} \Big|_{-\pi}^{\pi} = 0 \tag{26.3}$$

The Schrödinger equation

The wave functions for each system were evaluated by the Schrödinger equation to form a quantized energy equation. For particle in a box, the Hamiltonian operator will operate on the wave function by taking the partial derivative with respect to *x* (eq 27.1). The same wave function will be returned after the operation along with the wave function curvature information (eq 27.2). The eigenvalue produced from the operation is the electronic energy equation (eq 27.3). The full steps from equation 27.1 to equation 27.3 are shown in Appendix C. The energy equation shows that energy is quantized in discrete levels.

$$-\frac{\hbar^2}{2m} \frac{d^2}{dx^2} \sqrt{\frac{2}{L}} \sin\left(\frac{n\pi x}{L} + \frac{n\pi}{2}\right) = E_n \sqrt{\frac{2}{L}} \sin\left(\frac{n\pi x}{L} + \frac{n\pi}{2}\right) \tag{27.1}$$

$$-\frac{\hbar^2}{2m} \left(-\frac{n^2\pi^2}{L^2}\right) \sqrt{\frac{2}{L}} \sin\left(\frac{n\pi x}{L} + \frac{n\pi}{2}\right) = E_n \sqrt{\frac{2}{L}} \sin\left(\frac{n\pi x}{L} + \frac{n\pi}{2}\right) \tag{27.2}$$

$$E_n = \frac{h^2 n^2}{8mL^2} \tag{27.3}$$

For a particle on a ring, the Hamiltonian operator takes the partial derivative of the wave function with respect to ϕ (eq 28.1). After the operation, the original wave

function is returned, and the eigenvalue is the rotational electronic energy equation (eq 28.2-28.3).

$$-\frac{\hbar^2}{2mr^2}\frac{d^2}{d\phi^2}\sqrt{\frac{1}{2\pi}}e^{im_\ell\phi} = E_{m_\ell}\sqrt{\frac{1}{2\pi}}e^{im_\ell\phi} \quad (28.1)$$

$$-\frac{\hbar^2}{2mr^2}(-{m_\ell}^2)\sqrt{\frac{1}{2\pi}}e^{im_\ell\phi} = E_{m_\ell}\sqrt{\frac{1}{2\pi}}e^{im_\ell\phi} \quad (28.2)$$

$$E_{m_\ell} = \frac{\hbar^2{m_\ell}^2}{8m\pi^2r^2} \quad (28.3)$$

Transition Wavelength

For spectra such as an absorbance spectrum, the typical x-axis will be transition wavelength, so from the energies, one can calculate the transition energy, E_T. This is done by taking the difference between the upper energy, $E_{i+\Delta i}$, and lower energy, E_i, levels in the transition (eq 29). Using this transition energy, the transition wavelength, λ_T, can be calculated between the quantum levels formulated from the Schrödinger equation (eq 30). This determines the positions of transitions along the wave length axis of a spectrum.

$$E_T = E_{i+\Delta i} - E_i \quad (29)$$

$$\lambda_T = \frac{hc}{E_T} \quad (30)$$

Transition Dipole Moment Integral

Since the wavelength of any transition can be determined, the allowed transitions must be identified. All spectroscopic transitions are summarized by selection rules based on the approximation that the intensity of a transition is proportional to the square of the transition dipole moment integral (eq 20).[11] Each system's wave functions will be evaluated in the integrand to determine the corresponding selection rules and the theoretical intensity.

To allow for an integral solution that can be applied to any transition, the upper quantum state in the transition will be denoted as $n+\Delta n$ (eq 31). The electric dipole operator is x which represents the electric field induced by light on the x-axis. Equation 32.1-32.4 shows each part of this integral. The transition dipole moment integrands were evaluated with an odd transition such as $\Delta n=\{\pm1,3,5\ldots\}$ and an even transition such as $\Delta n= \{\pm2,4,6\ldots\}$. For the sine arguments, both functions will sum to zero. This is found since sine of a π multiple and sine of zero both give a zero output (eq 32.1 & 32.3). For the cosine arguments if the Δn is even, the cosine function is 0 as an even π multiple will give a 1 output which will cancel out during evaluation (eq 32.2 & 32.4). If the Δn is odd, the cosine function is non-zero as the cosine of an odd π multiple and the cosine of zero will give the same output of opposing values (eq 32.2 & 32.4). Therefore, only the odd transitions will give a non-zero integral, and the even transitions will give a zero integral (eq 33-34). The full set of calculations are shown in Appendix D.

$$\int_{-L/2}^{L/2}\sqrt{\frac{2}{L}}\sin\left(\frac{n\pi x}{L}+\frac{n\pi}{2}\right)*x*\sqrt{\frac{2}{L}}\sin\left(\frac{(n+\Delta n)\pi x}{L}+\frac{(n+\Delta n)\pi}{2}\right)dx \quad (31)$$

$$=\left[-\frac{x}{\Delta n\pi}\sin\left(-\frac{\Delta n\pi x}{L}-\frac{\Delta n\pi}{2}\right)\Big|_{-\frac{L}{2}}^{\frac{L}{2}}+\right. \quad (32.1)$$

$$\frac{L}{\Delta n^2\pi^2}\cos\left(-\frac{\Delta n\pi x}{L}-\frac{\Delta n\pi}{2}\right)\Big|_{-\frac{L}{2}}^{\frac{L}{2}}+ \quad (32.2)$$

$$-\frac{x}{2n\pi+\Delta n\pi}\sin\left(\frac{2n\pi x+\Delta n\pi x}{L}+\frac{2n\pi+\Delta n\pi}{2}\right)\Big|_{-\frac{L}{2}}^{\frac{L}{2}}+ \quad (32.3)$$

$$\left.-\frac{L}{(2n\pi+\Delta n\pi)^2}\cos\left(\frac{2n\pi x+\Delta n\pi x}{L}+\frac{2n\pi+\Delta n\pi}{2}\right)\Big|_{-\frac{L}{2}}^{\frac{L}{2}}\right] \quad (32.4)$$

$$\langle n|\mu|n\pm\Delta n_{odd}\rangle = -\frac{2L}{\Delta n^2\pi^2}+\frac{2L}{(2n\pi+\Delta n\pi)^2} \quad (33)$$

$$\langle n|\mu|n\pm\Delta n_{even}\rangle = 0 \quad (34)$$

The following are integral findings for particle on a ring. The electric dipole for this system is cos ϕ, as is simulates the positive and negative values of the electric field of light oscillating through the ring (eq 35). The transition moment integrands were evaluated with an odd transition such as Δm_ℓ ={1,3,5…}(eq 36) and an even transition such as Δm_ℓ ={±2,4,6…}(eq 37). With particle on a ring both even and odd transitions went to zero therefore a breakdown to individual integers was necessary. To further investigate, equation 38.1 shows a vital step within solving for the integral. Only if Δm_ℓ = ± 1, will the final evaluation step include the arguments in equation 38.2 which go to ½ and zero respectively. Therefore, only Δm_ℓ = ± 1 transitions are allowed at a constant integral of ½ (eq 38.3). This gives a Δm_ℓ = ± 1 selection rule. The full set of calculations are shown in Appendix D.

$$\int_{-\pi}^{\pi} \sqrt{\frac{1}{2\pi}} e^{-im_\ell \phi} \cos(\phi) \sqrt{\frac{1}{2\pi}} e^{i(m_\ell + \Delta m_\ell)\phi} d\phi \quad (35)$$

$$\langle m_\ell | \mu | m_\ell \pm \Delta m_{\ell(odd)} \rangle = 0 \quad (36)$$

$$\langle m_\ell | \mu | m_\ell \pm \Delta m_{\ell(even)} \rangle = 0 \quad (37)$$

$$\frac{1}{2\pi} \int_{-\pi}^{\pi} \cos(\phi) \cos(\Delta m_\ell \phi)\, d\phi + \frac{1}{2\pi} \int_{-\pi}^{\pi} \cos(\phi)\, i \sin(\Delta m_\ell \phi)\, d\phi \quad (38.1)$$

$$\frac{1}{4\pi}\phi \Big|_{-\pi}^{\pi} - \frac{1}{8\pi}\cos(2\phi) \Big|_{-\pi}^{\pi} \quad (38.2)$$

$$\langle m_\ell | \mu | m_\ell \pm 1 \rangle = \frac{1}{2} \quad (38.3)$$

Transition Moment Integral

With the scattering processes, a second photon is introduced to the electric dipole and therefore becomes a second order operator, modeled by x^2 for particle in a box (eq 39.1). Raman anti-stokes scattered photons are those that have a higher leaving frequency and show a transition decrease in quantum level (-Δn), Stokes lines are those that have a

lower leaving frequency and show a transition increase in quantum level and (+Δn). Rayleigh lines are elastic scattered photons that have the same leaving frequency and transition quantum level does not change ($\Delta n=0$).[10] The transition moment integrands were evaluated for integrals with odd Raman scattering (eq 40), even Raman scattering (eq 41), and Rayleigh scattering (eq 42.3). Equations 39.2-39.4 show the arguments in the evaluation step of this integral. The sine arguments all go to zero with a π multiple or zero inside each function (eq 39.2-39.3). The cosine arguments with an odd Δn gives a zero integral since the evaluation from $^{L}/_{2}$ to $^{-L}/_{2}$ will give the same value therefore cancelling each other out (eq 38). The cosine arguments with an even Δn gives a non-zero output since the evaluation from $^{L}/_{2}$ to $^{-L}/_{2}$ will give the same values but with different signs (eq 39). It can be concluded that particle in a box even Raman scattering are allowed and odd Raman scattering are not allowed. This gives the selection rules of Δn ={ ± 2,4,6…}. The full set of calculations are shown in Appendix E.

$$\int_{-L/2}^{L/2}\sqrt{\frac{2}{L}}\sin\left(\frac{n\pi x}{L}+\frac{n\pi}{2}\right)*x^2*\sqrt{\frac{2}{L}}\sin\left(\frac{(n+\Delta n)\pi x}{L}+\frac{(n+\Delta n)\pi}{2}\right)dx \quad (39.1)$$

$$\frac{x^2}{\Delta n\pi}\sin\left(\frac{\Delta n\pi x}{L}+\frac{\Delta n\pi}{2}\right)+\frac{2L^2}{(2n\pi+\Delta n\pi)^3}\sin\left(\frac{2n\pi x}{L}+n\pi+\frac{\Delta n\pi x}{L}+\frac{\Delta n\pi}{2}\right)\Big|_{-\frac{L}{2}}^{\frac{L}{2}} \quad (39.2)$$

$$-\frac{2L^2}{\Delta n^3\pi^3}\sin\left(\frac{\Delta n\pi x}{L}+\frac{\Delta n\pi}{2}\right)-\frac{x^2}{2n\pi+\Delta n\pi}\sin\left(\frac{2n\pi x}{L}+n\pi+\frac{\Delta n\pi x}{L}+\frac{\Delta n\pi}{2}\right)\Big|_{-\frac{L}{2}}^{\frac{L}{2}} \quad (39.3)$$

$$\frac{2Lx}{\Delta n^2\pi^2}\cos\left(\frac{\Delta n\pi x}{L}+\frac{\Delta n\pi}{2}\right)-\frac{2Lx}{(2n\pi+\Delta n\pi)^2}\cos\left(\frac{2n\pi x}{L}+n\pi+\frac{\Delta n\pi x}{L}+\frac{\Delta n\pi}{2}\right)\Big|_{-\frac{L}{2}}^{\frac{L}{2}} \quad (39.4)$$

$$\langle n|x^2|n\pm\Delta n_{odd}\rangle=0 \quad (40)$$

$$\langle n|x^2|n\pm\Delta n_{even}\rangle=\frac{2L^2}{\Delta n\pi}-\frac{2L^2}{(2n\pi+\Delta n\pi)^2} \quad (41)$$

Rayleigh scattering is determined with an equation without the Δn as it is set to zero in elastic scattering (eq 42.1). In the evaluation equation, the sine functions both go

to zero with the argument inside the function being zero or a π multiple (eq 42.2). The first argument will give length divided by a constant, and the cosine function produces the rest of the final integral output (eq 42.3). The full set of calculations are shown in Appendix E.

$$\int_{-L/2}^{L/2} \sqrt{\frac{2}{L}} \sin\left(\frac{n\pi x}{L} + \frac{n\pi}{2}\right) * x^2 * \sqrt{\frac{2}{L}} \sin\left(\frac{n\pi x}{L} + \frac{n\pi}{2}\right) dx \qquad (42.1)$$

$$\frac{2x}{L} + \frac{x^2}{2n\pi} \sin\left(\frac{2n\pi x}{L} + n\pi\right) - \frac{2Lx}{(2n\pi)^2} \cos\left(\frac{2n\pi x}{L} + n\pi\right) + \frac{2L^2}{(2n\pi)^3} \sin\left(\frac{2n\pi x}{L} + n\pi\right)\Big|_{-\frac{L}{2}}^{\frac{L}{2}} \qquad (42.2)$$

$$\langle n|x^2|n\rangle = \frac{L^2}{3} - \frac{L^2}{2n^2\pi^2} \qquad (42.3)$$

For the particle on a ring, the transition moment integrands were also evaluated with odd Raman scattering (eq 43), even Raman scattering (eq 44), and Rayleigh scattering (eq 45). Just as with the single photon system, both odd and even transition integrals went to zero. At equation 46.1 inspecting individual integers, only the $\Delta m_\ell = \pm 2$ transitions were non-zero (eq 46.2-46.3). This lends to the selection rules $\Delta m_\ell = \pm 2$. Each integral solution is shown in Appendix E.

$$\int_{-\pi}^{\pi} \sqrt{\frac{1}{2\pi}} e^{-im_\ell\phi} * \cos^2\phi * \sqrt{\frac{1}{2\pi}} e^{i(m_\ell + \Delta m_\ell)\phi} d\phi \qquad (43)$$

$$\langle m_\ell|\hat{\alpha}|m_\ell \pm \Delta m_{\ell(odd)}\rangle = 0 \qquad (44)$$

$$\langle m_\ell|\hat{\alpha}|m_\ell \pm \Delta m_{\ell(even)}\rangle = 0 \qquad (45)$$

$$\int_{-\pi}^{\pi} \cos(\Delta m_\ell\phi)\cos(\phi)\, d\phi \qquad (46.1)$$

$$\frac{\phi}{8\pi}\Big|_{-\pi}^{\pi} - \frac{1}{32\pi}\sin(4\phi)\Big|_{-\pi}^{\pi} \qquad (46.2)$$

$$\langle m_\ell|\hat{\alpha}|m_\ell \pm 2\rangle = \frac{1}{4} \qquad (46.3)$$

Rayleigh scattering is the application of the same starting equation with the Δm_ℓ set to zero (eq 47.1). In the final evaluation step, the first argument gives the constant ½ and the sine function goes to zero as the inside of the function is always a π multiple (eq 47.2). The full set of calculations are in Appendix E.

$$\int_{-\pi}^{\pi} \sqrt{\frac{1}{2\pi}} e^{-im_\ell \phi} * \cos^2 \phi * \sqrt{\frac{1}{2\pi}} e^{im_\ell \phi} d\phi \tag{47.1}$$

$$\frac{\phi}{4\pi}\Big|_{-\pi}^{\pi} + \frac{1}{8\pi}\sin(2\phi)\Big|_{-\pi}^{\pi} \tag{47.2}$$

$$\langle m_\ell | \hat{\alpha} | m_\ell \rangle = \frac{1}{2} \tag{47.3}$$

CHAPTER III

Numerical Solution

A numerical solution is an algebraic approximate solution which models the system of interest. In this case a spreadsheet has been used to evaluate the Schrödinger equation and the transition dipole moment or transition moment integrals. The advantage to using a spreadsheet is the ability to produce a dynamic theoretical spectrum. With the ability to calculate multiple spectral transitions simultaneously, the spreadsheet shows the trends and variable relationships.

Spreadsheet wave functions

Wave functions are formed on a spreadsheet by calculating the desired normalized equation using *dx* as increments between values. The following figures pertain to the particle in a box system. The particle in a box shifted wave functions used throughout the analytical solution is plotted for $n=\{1,2,\&3\}$ in *Figure 7*. *Figure 8* shows the same set of wave functions in a smaller box.

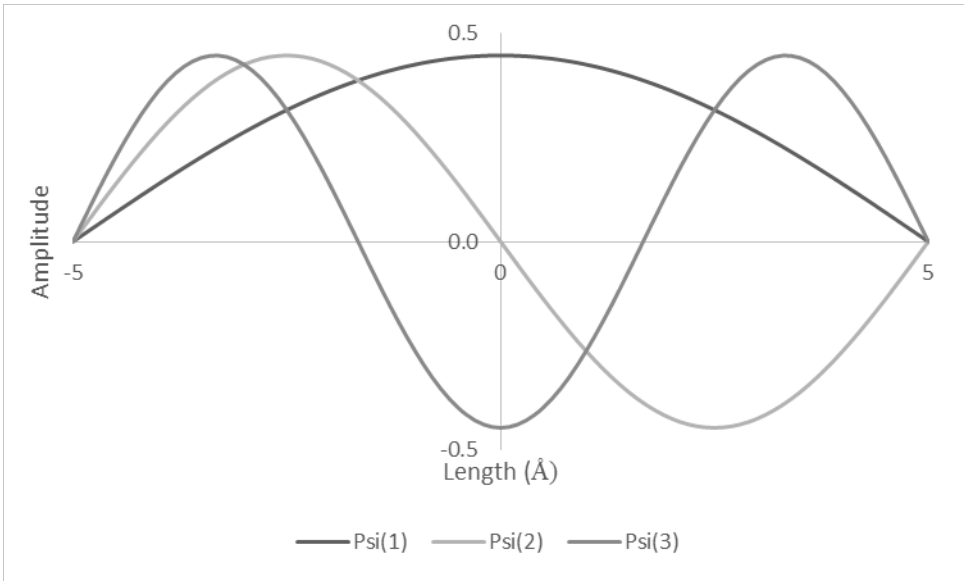

Figure 7. Numerical wave function for particle in a box for energy levels (*n*) 1-3 in a 10Å box.

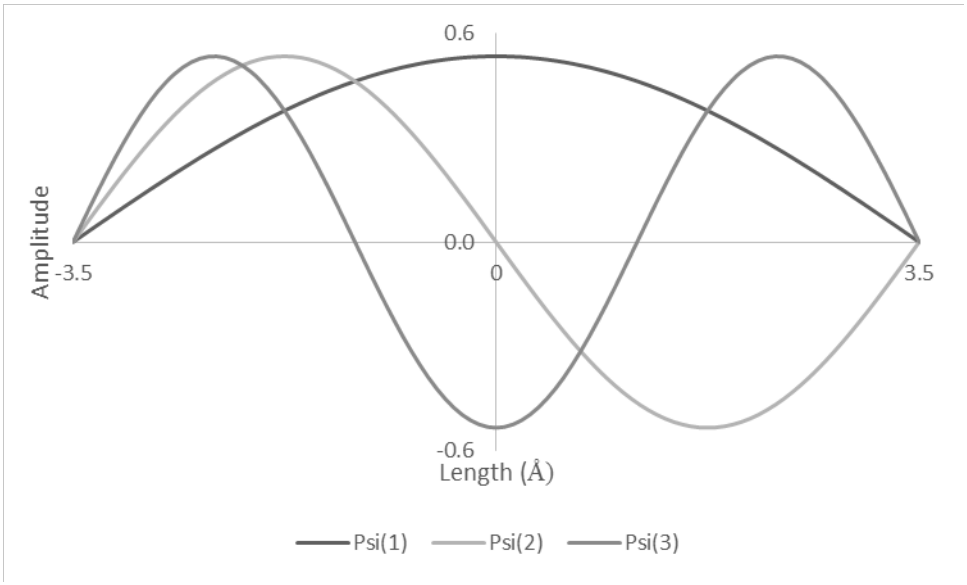

Figure 8. Numerical wave function for particle in a box for energy levels (*n*) 1-3 in a 7Å box.

The following figures pertain to the particle on a ring system. *Figure 9* shows the first three wave functions. There is a quantum level of zero for rotational levels unlike that of the particle in a box levels. This level has no particle rotational movement and therefore will have no rotational energy. *Figure 10* shows the same wave functions with a smaller radius at 5Å.

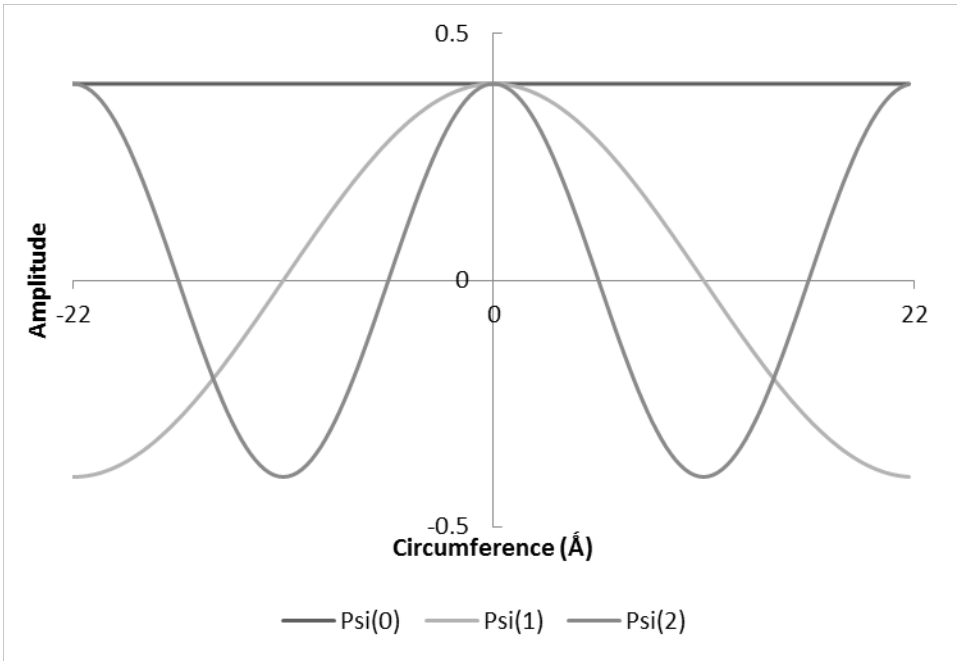

Figure 9. Numerical plotted wave function for particle on a 7Å ring for rotational levels 0-2.

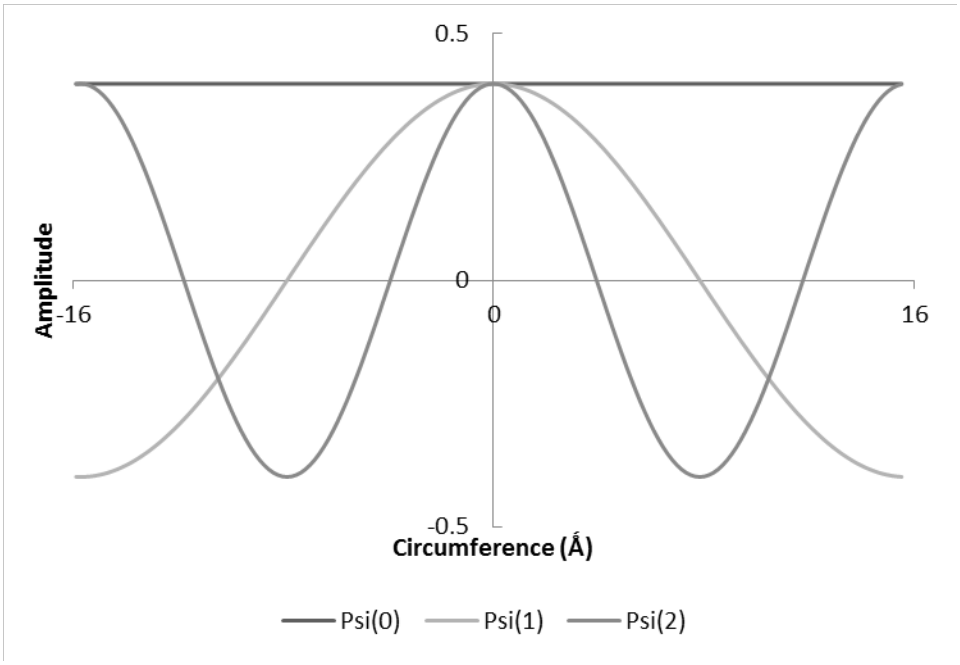

Figure 10. Numerical plotted wave function for particle on a 5Å ring for rotational levels 0-2.

Orthonormality

To demonstrate the orthonormality conditions, an integral is obtained numerically by calculating the Riemann sums over all product combinations of the wave functions. Equation 48 is the numerical equation for the orthonormality matrix. Several wave functions, in this case 15, will be on one sheet with 100 increments on the x-axis. They will form a 100x15 matrix of data. By multiplying the transpose of this matrix by the same matrix and the change in *x* increment, a matrix of numerical integrals is produced showing the normalization and orthogonality of all 15 wave functions. *Figure 11* and *Figure 12* depict the action in the spreadsheet to numerically solve for an integral.

$$\delta_{n,m} = \sum_{-L/2}^{+L/2} \left(\psi_n^*(x)\psi_m(x)\right)\Delta x \qquad (48)$$

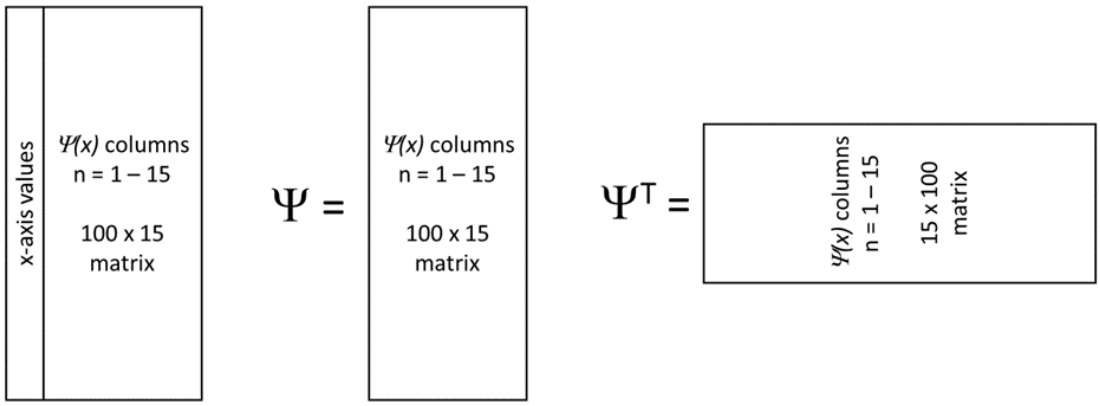

Figure 11. Spreadsheet wave function and transposed wave function depiction.

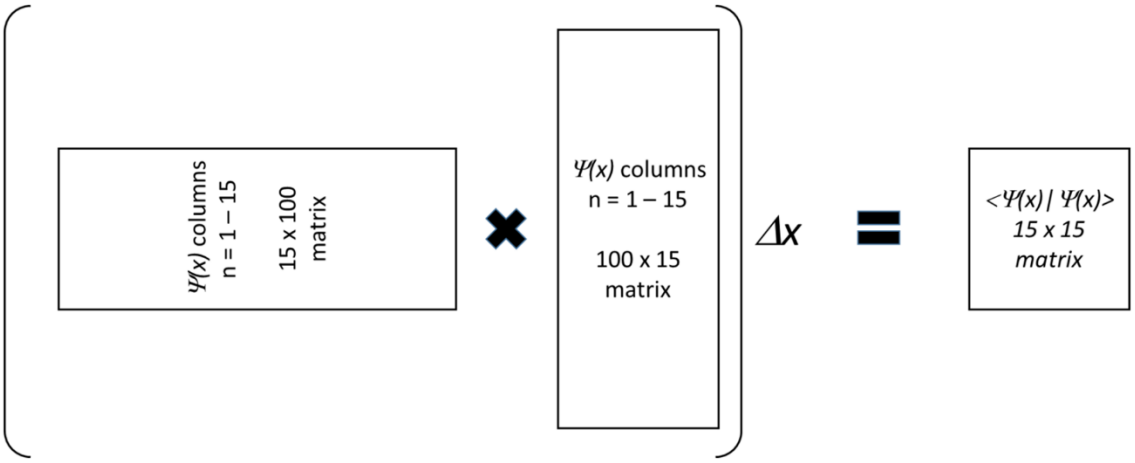

Figure 12. Spreadsheet integration depiction.

Table 1 show the orthonormality matrix given for particle in a box and particle on a ring. Where the same quantum numbers cross in the table, there is an output of 1.00 showing normalization. All other crosses have an output of 0.00 showing the wave function orthogonality.

Table 1

Orthonormality Matrix Output for a particle in a 10Å box and particle on a 5Ǻ ring

n/n	1	2	3	4	5	6
1	1.00	0.00	0.00	0.00	0.00	0.00
2	0.00	1.00	0.00	0.00	0.00	0.00
3	0.00	0.00	1.00	0.00	0.00	0.00
4	0.00	0.00	0.00	1.00	0.00	0.00
5	0.00	0.00	0.00	0.00	1.00	0.00
6	0.00	0.00	0.00	0.00	0.00	1.00

Schrödinger's equation

To determine spectral transition wavelength, the quantized energy is calculated from the Schrödinger equation. In order to easily calculate the energy, the Schrödinger equation will be rearranged (eq 49.1-49.3).

$$\hat{H}\psi_n(x) = E_n\psi_n(x) \qquad (49.1)$$

$$\langle \psi_n(x) | \widehat{H} | \psi_n(x) \rangle = E_n \langle \psi_n(x) | \psi_n(x) \rangle \quad (49.2)$$

$$E_n = \langle \psi_n(x) | \widehat{H} | \psi_n(x) \rangle \quad (49.3)$$

Just as with the orthonormality equation, the energy equation (eq 49.3) is transformed to a numerical form (eq 50). A slight adjustment to the Hamiltonian will give the numerical equation for the particle on a ring (eq 51).

$$E_n = -\frac{h^2}{8m\pi^2} \sum_{-L/2}^{+L/2} \left(\psi_n^*(x) \frac{d}{dx} \frac{d}{dx} \psi_n(x) \right) \Delta x \quad (50)$$

$$E_{m_\ell} = -\frac{h^2}{8mr^2\pi^2} \sum_{-\pi}^{\pi} \left(\psi_{m_\ell}^*(\phi) \frac{d}{d\phi} \frac{d}{d\phi} \psi_{m_\ell}(\phi) \right) \Delta\phi \quad (51)$$

Since a derivative is the slope of a tangent line, the slope can be taken twice to produce a second derivative. This can be applied through the centered slope method (eq 52-53). In this method, the slope is calculated across two intervals, divided by two Δx increments and plotted on the midpoint of the difference. Equation 52 leads to the first derivative, ψ'_n, and done a second time will produce the second derivative, ψ''_n (eq 52-55). Each equation will form another plotted sheet and output (*Figure 13*-*Figure 16*).

$$\psi'_n = \frac{d}{dx} \psi_n(x) = \frac{\psi_n(x+\Delta x) - \psi_n(x-\Delta x)}{2\Delta x} \quad (52)$$

$$\psi''_n = \frac{d}{dx} \psi'_n(x) = \frac{\psi'_n(x+\Delta x) - \psi'_n(x-\Delta x)}{2\Delta x} \quad (53)$$

These same equations are applied to the particle on a ring system.

$$\psi'_{m_\ell} = \frac{d}{d\phi} \psi_{m_\ell}(\phi) = \frac{\psi_{m_\ell}(\phi+\Delta\phi) - \psi_{m_\ell}(\phi-\Delta\phi)}{2\Delta\phi} \quad (54)$$

$$\psi''_{m_\ell} = \frac{d}{d\phi} \psi'_{m_\ell}(\phi) = \frac{\psi_{m_\ell}(\phi+\Delta\phi) - \psi_{m_\ell}(\phi-\Delta\phi)}{2\Delta\phi} \quad (55)$$

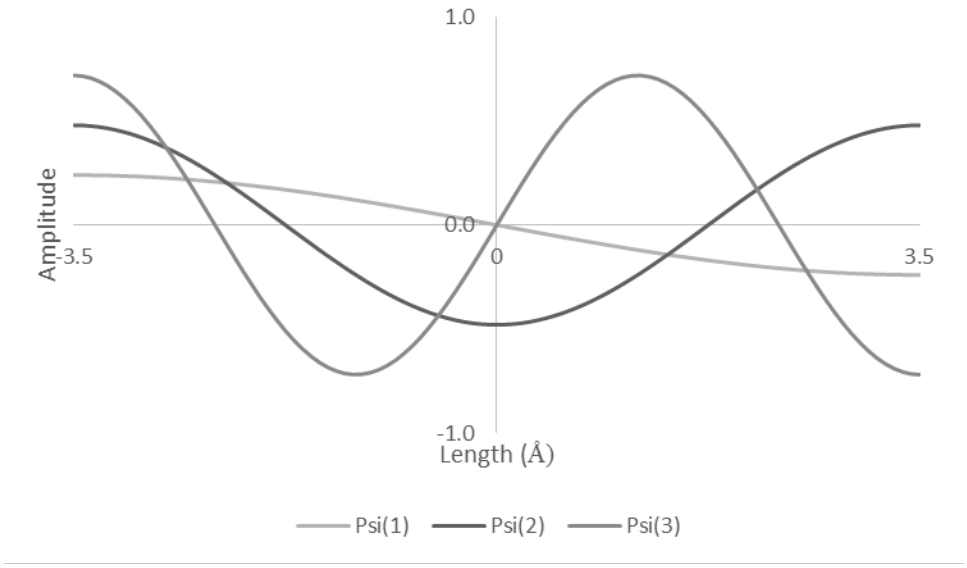

Figure 13. First derivative (prime) wave function for particle in a 7Å box.

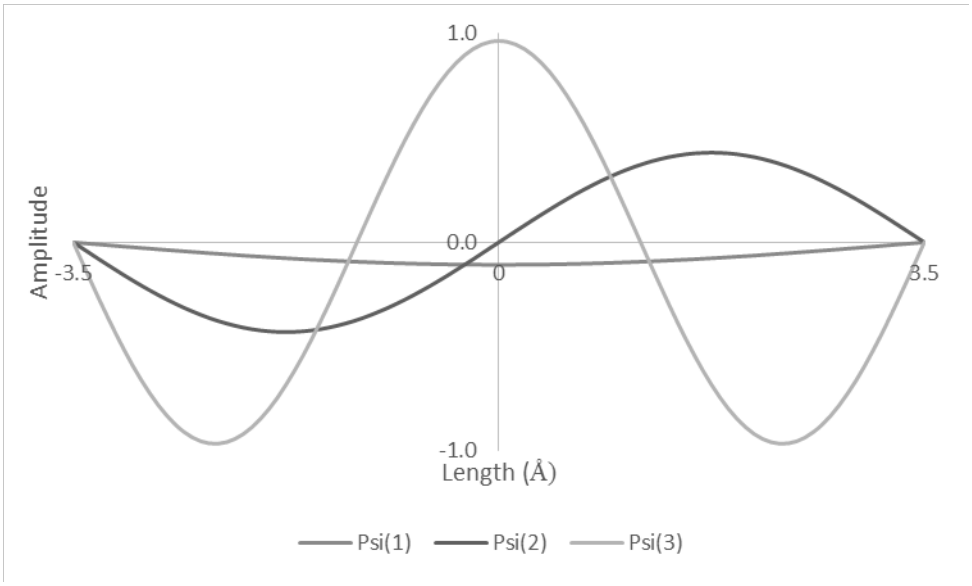

Figure 14. Second derivative (double prime) wave function for particle in a 7Å box.

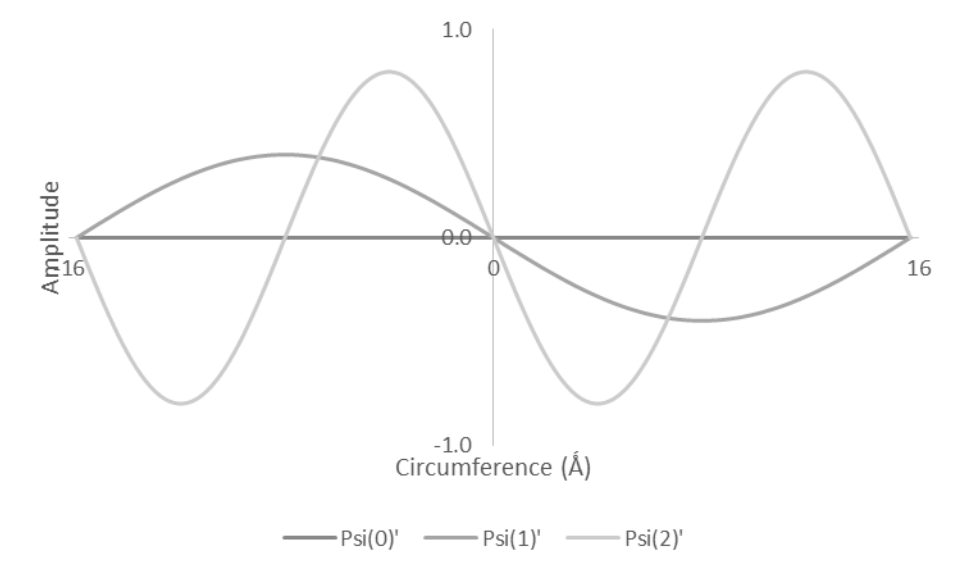

Figure 15. First derivative (prime) wave function for particle on a ring with a 5Å radius.

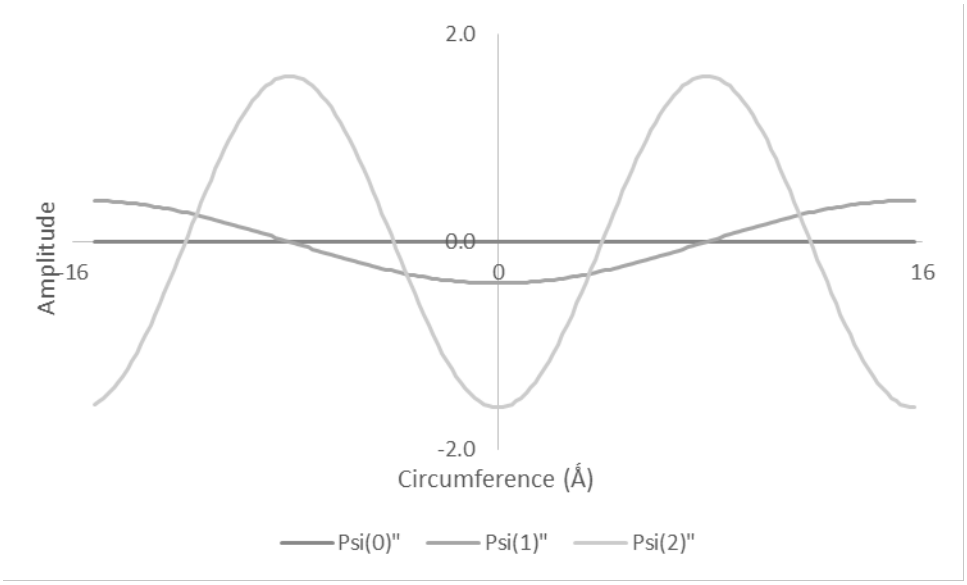

Figure 16. Second derivative (double prime) wave function for particle on a ring with a 5Å radius.

To calculate equation 50 and 51 in the spreadsheet, the transposed matrix of wave functions and the matrix of double prime wave functions will be multiplied and summed through matrix multiplication. The calculated matrix will give the energy eigenvalues of

each quantum state on the corresponding diagonal (Table 2-Table 3). The unit reported in this example as *kJ/mol*.

Table 2

Energy Matrix Output for Particle in a 7Å Box in kJ/mol

n/n	**1**	**2**	**3**	**4**	**5**	**6**
1	74.08	0.00	0.00	0.00	0.00	0.00
2	0.00	296.01	0.00	0.00	0.00	0.00
3	0.00	0.00	664.93	0.00	0.00	0.00
4	0.00	0.00	0.00	1179.37	0.00	0.00
5	0.00	0.00	0.00	0.00	1837.32	0.00
6	0.00	0.00	0.00	0.00	0.00	2636.16

Table 3

Energy Matrix Output for Particle on a Ring with a 7Å radius in kJ/mol

m_ℓ/m_ℓ	**0**	**1**	**2**	**3**	**4**	**5**
0	0.00	0.00	0.00	0.00	0.00	0.00
1	0.00	7.50	0.00	0.00	0.00	0.00
2	0.00	0.00	29.98	0.00	0.00	0.00
3	0.00	0.00	0.00	67.32	0.00	0.00
4	0.00	0.00	0.00	0.00	119.35	0.00
5	0.00	0.00	0.00	0.00	0.00	185.80

Numerical Error

At this point, the analytical and numerical energies can be compared to see the accuracy of the numerical method (Table 4-Table 5). There is a negative bias to the error that increases with quantum number.

Table 4

Analytical and Numerical comparison for Particle in a 7Å Box

Quantum Number	**Analytical Solution**	**Numerical Solution**	**Difference**	**% Error**

1	74.10	74.08	-2.44E-02	-0.03%
2	296.40	296.01	-3.90E-01	-0.13%
5	1852.50	1837.32	-1.52E+01	-0.82%
10	7410.02	7169.42	-240.59	-3.25%
15	16672.53	15474.37	-1198.16	-7.19%

Table 5

Analytical and Numerical comparison for Particle on a ring with a 7Å radius

Quantum Number	Analytical Solution	Numerical Solution	Difference	% Error
0	0.00	0.00	-0.00E+00	-0.00%
1	7.51	7.50	-3.05E-03	-0.04%
2	30.03	29.98	-4.88E-02	-0.16%
5	187.70	185.80	-1.90E+00	-1.01%
10	750.79	720.79	-3.00E+01	-4.00%
11	908.46	864.68	-4.38E+01	-4.82%
15	1689.28	1540.44	-1.49E+02	-8.81%

Boltzmann distribution and Transition Dipole Integral

The intensity of the transition wavelengths will be approximated with the transition moment integral combined with the Boltzmann distribution. The Boltzmann distribution shows the population of molecules in a certain energy state.[12] The population of a level is dependent on the temperature, T, of the system, the energy, E_n, of the level compared to the ground state energy E_1, and the degeneracy of the level, g_n compared to the ground state degeneracy g_1 (eq 56).[12] For a particle in a box the ground state will be n=0 and m_ℓ=0 for a particle on a ring. The particle in a box system will have a degeneracy of 1 with every quantum state, and the particle on a ring system will have a degeneracy of 2 for all $m_\ell \neq 0$.

$$B = \frac{g_n}{g_1} e^{-\frac{E_n - E_1}{kT}} \tag{56}$$

When the Boltzmann distribution is combined with the transition dipole moment integral squared, there is a relatively reasonable theoretical intensity value (eq 57-58).

$$I \propto B\langle n'|\mu|n\rangle^2 \quad (57)$$

$$I \propto B\langle m_\ell'|\mu|m_\ell\rangle^2 \quad (58)$$

For the particle in a box, the x-axis will be used as the electric dipole operator producing a wave function that is perturbed by the oscillating dipole. For the particle on ring, $\cos(\phi)$ will mimic light as it oscillates through the ring.[10] The following are the previous wave functions shown in *Figure 7* and *Figure 9* modified by the electric dipole operator (*Figure 17-Figure 18*).

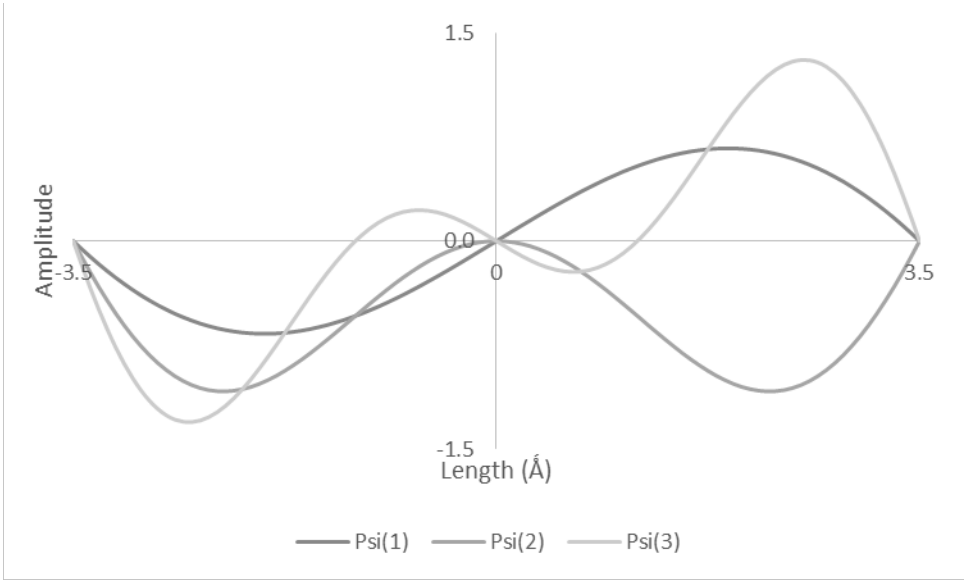

Figure 17. Electric dipole modified wave function for particle in a 7Å box.

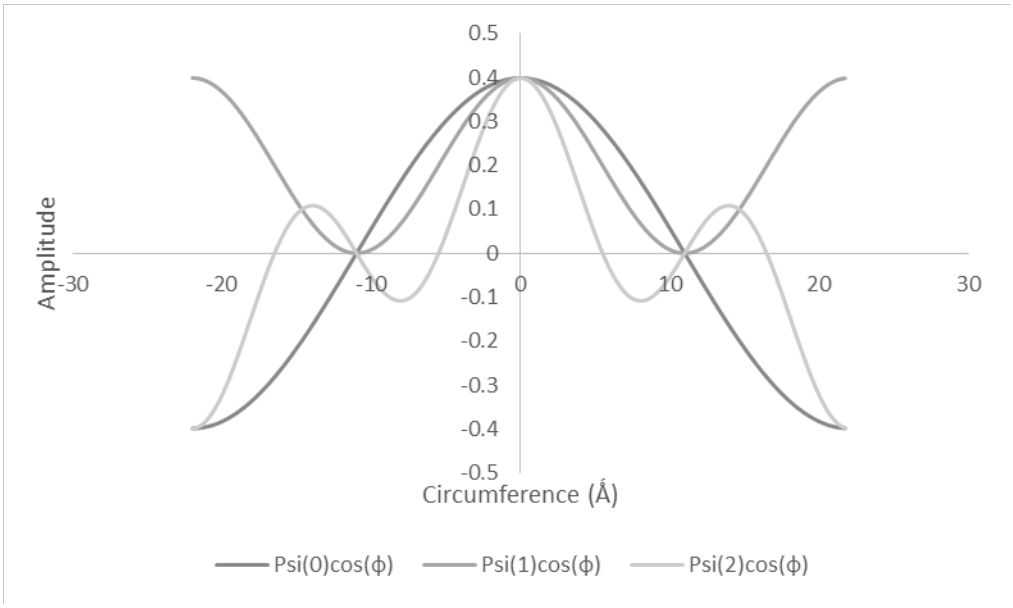

Figure 18. Electric dipole modified wave function for particle on a ring with a 7Å radius.

In order to calculate the transition moment integral, the original wave function matrix and the electric dipole modified wave function matrix will be matrix multiplied and squared to give the transition intensity. The produced matrix will give the approximation for all the energy level transitions (Table 6-Table 8). The selection rules for the transition are evident as all allowed transitions have a non-zero intensity. The following table clearly shows the $\Delta n = \{\pm 1,3,5\ldots\}$ selection rule. Table 7 shows the same particle in a smaller 7Å box.

Table 6

Transition Dipole Moment Integral squared for a Particle in a 100Å Box

n/n	**1**	**2**	**3**	**4**	**5**	**6**
1	0.00	324	0.00	2.08	0.00	0.16
2	324	0.00	378	0.00	3.38	0.00
3	0.00	378	0.00	394	0.00	4.01
4	2.08	0.00	394	0.00	400	0.00
5	0.00	3.38	0.00	400	0.00	403
6	0.160	0.00	4.01	0.00	403	0.00

Table 7

Transition Dipole Moment Integral squared for a Particle in a 7Å Box

n/n	1	2	3	4	5	6
1	0.00	1.59	0.00	0.01	0.00	0.001
2	1.59	0.00	1.85	0.00	0.02	0.00
3	0.00	1.85	0.00	1.93	0.00	0.02
4	0.01	0.00	1.93	0.00	1.96	0.00
5	0.00	0.02	0.00	1.96	0.00	1.98
6	0.001	0.00	0.02	0.00	1.98	0.00

For particle on a ring, the table clearly shows the $\Delta m_\ell = \pm 1$ selection rule. The integral output is the same for every allowed transition at ¼ (Table 8).

Table 8

Transition Dipole Integral squared for a Particle on Ring with a 7Å and a 5Å radius

m_ℓ/m_ℓ	0	1	2	3	4	5
0	0.00	0.25	0.00	0.00	0.00	0.00
1	0.25	0.00	0.25	0.00	0.00	0.00
2	0.00	0.25	0.00	0.25	0.00	0.00
3	0.00	0.00	0.25	0.00	0.25	0.00
4	0.00	0.00	0.00	0.25	0.00	0.25
5	0.00	0.00	0.00	0.00	0.25	0.00

Simulated Spectrum

The information so far will produce a stick spectrum. For particle in a box, these transitions and stick spectrum lend to producing an absorption spectrum (*Figure 19*). All instruments have a spectral band width. In order to simulate an instrumental spectrum, a Gaussian distribution is placed around each transition (eq 61), and a final sum of all the transitions will show a realistic absorption spectrum (*Figure 20*). The absorption of each transition is represented by the product of the Boltzmann distribution, the square of the transition dipole integral, and the Gaussian distribution (eq 59-61).

$$B_n = \frac{g_n}{g_1} e^{-\frac{E_n - E_1}{kT}} \tag{59}$$

$$I_{n\to n'} = (\psi_{n'}^T x \psi_n \Delta x)^2 \tag{60}$$

$$G_{n\to n'} = \frac{1}{\Delta\lambda\sqrt{2\pi}} e^{-\left(\frac{\lambda-\lambda_{n\to n'}}{\Delta\lambda\sqrt{2\pi}}\right)^2} \tag{61}$$

$$A_{n\to n'}^{Gaussian} = B_n I_{n\to n'} G_{n\to n'} \tag{62}$$

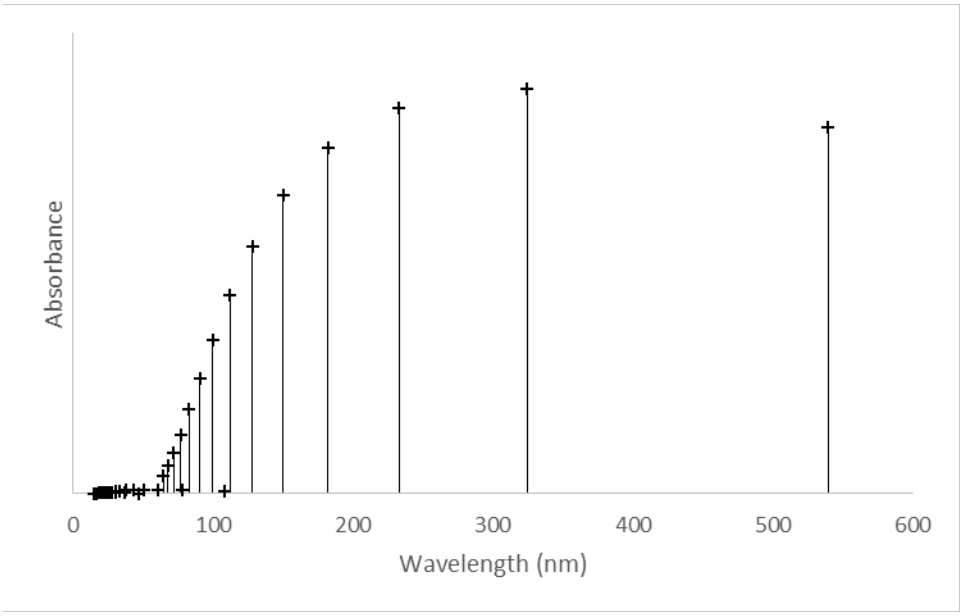

Figure 19. Stick spectrum for a particle in a 7Å box at 50000K.

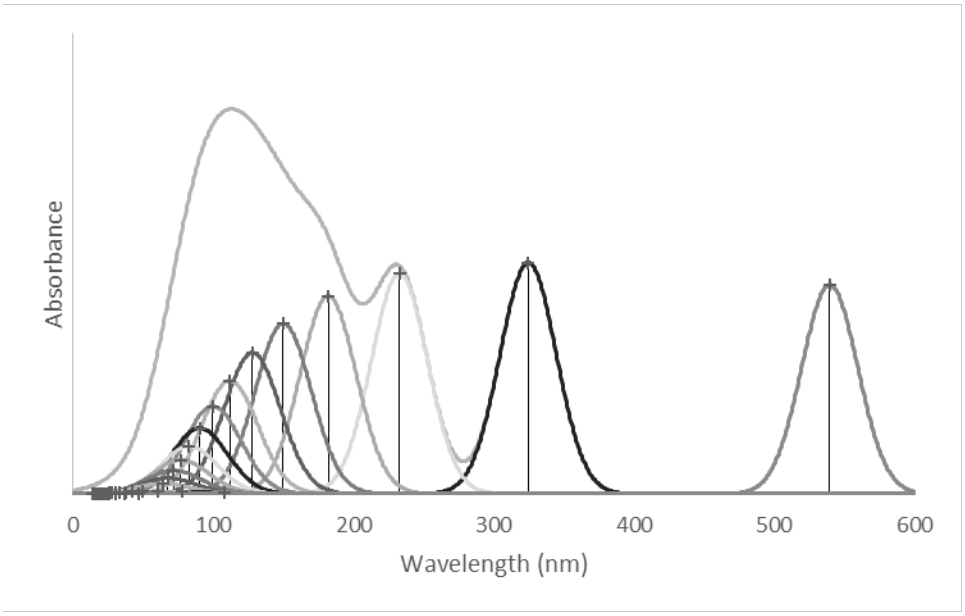

Figure 20. Theoretical Absorption spectrum convolved with individual transitions for a particle in a 10Å box at 50000K.

Summing up the contributions from each transition at each wavelength produces a theoretical absorption spectrum (*Figure 21*). This is the realistic output one would expect from an instrumental spectrum.

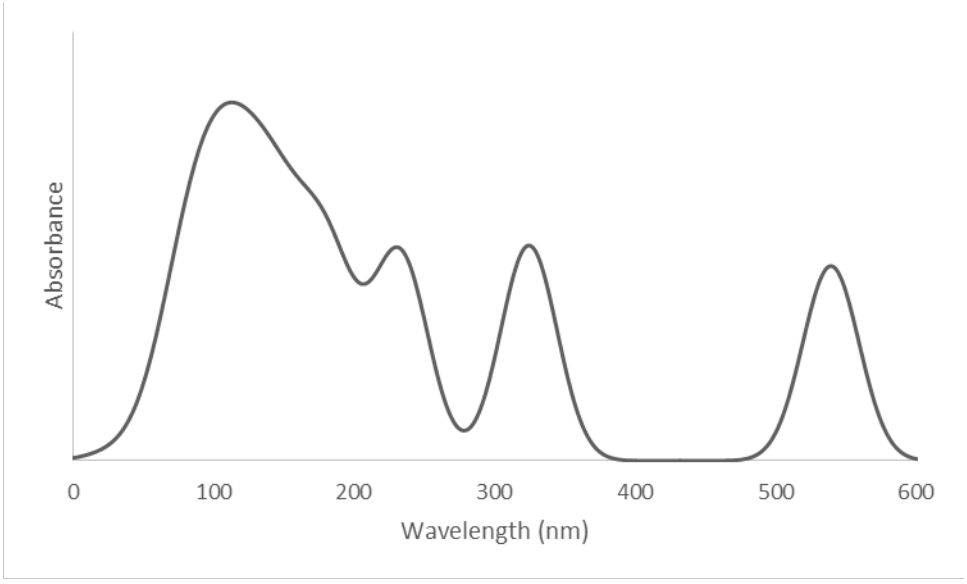

Figure 21. Theoretical absorption spectrum for a particle in a 7Å box at 50000K.

Pure rotational spectra is classically plotted with wavenumber as the x-axis, so for the particle on a ring theoretical spectra we will plot wavenumber instead of wavelength versus intensity (*Figure 23*).

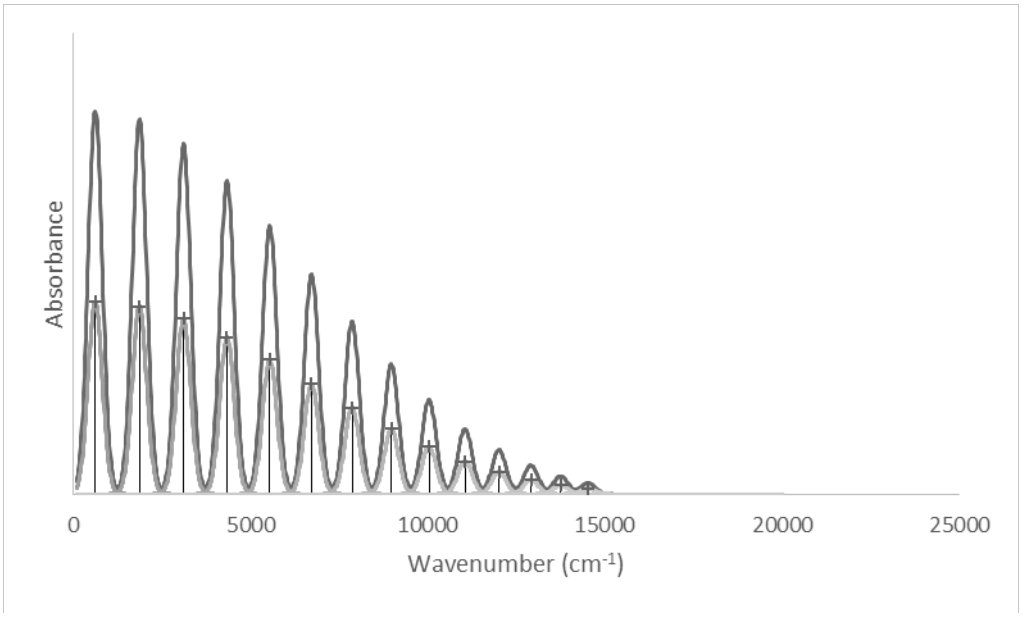

Figure 22. Theoretical absorption spectrum convolved with individual transitions for particle on a ring with a 7Å radius at 6000K.

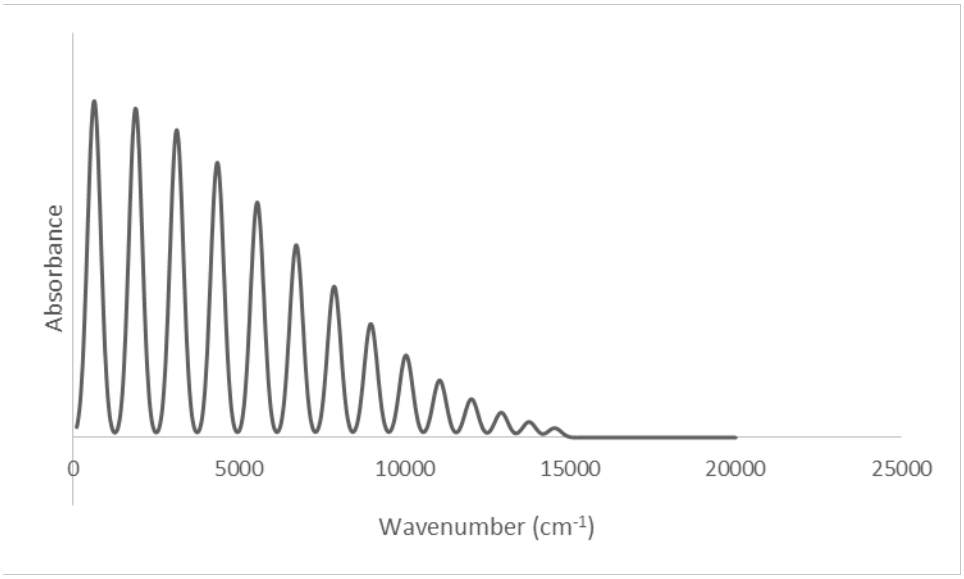

Figure 23. Theoretical absorption spectrum for a particle on a ring with a 7Å radius at 6000K.

Transition Moment Integral

Rayleigh and Raman scattering is a two photon system where elastic scattering returns to the same quantum state and inelastic scattering returns to a different quantum state.[12] The Raman/ Rayleigh two photon process may also be simulated by adding polarizability in the form of a second order electric dipole. This time the wave function will be perturbed twice by the x-axis (*Figure 24*).

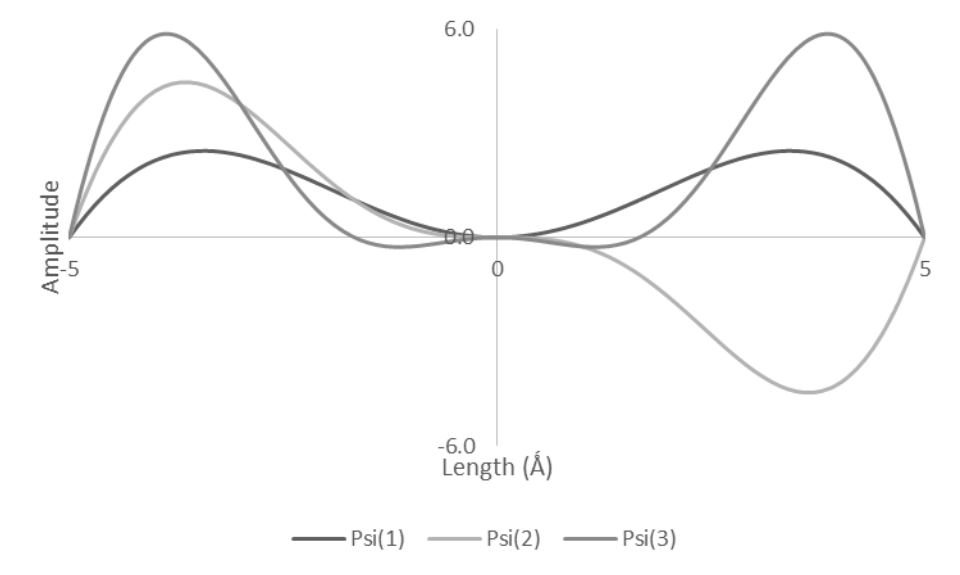

Figure 24. Raman electric dipole modified wave function for a particle in a 10Å box.

The Raman electric dipole modified wave functions and the original wave functions will again be integrated via matrix multiplication to solve the transition moment integral. The matrix gives the intensities for each of the energy levels. The particle in a box Raman selection rules are evident at $\Delta n=\{\pm 0,2,4,6\ldots\}$ as they produce a non-zero result (Table 9). The Rayleigh intensities lie on the $\Delta n=0$ diagonal which are allowed at every quantum level.

Table 9

Raman Transition Moment Integral squared for a Particle in a 10Å Box

n/n	1	2	3	4	5	6
1	107000	0.0000	144000	0.0000	4950	0.0000
2	0.0000	499000	0.0000	203000	0.0000	9020
3	144000	0.0000	604000	0.0000	226000	0.0000
4	0.0000	203000	0.0000	643000	0.0000	237000
5	4950	0.0000	225570.43	0.0000	661000	0.0000
6	0.0000	9020	0.0000	237000	0.0000	671000

The particle on a ring Raman selection rules are evident at $\Delta m_\ell \pm 2$ and again stay constant (Table 10). The Rayleigh intensities are along the $\Delta m_\ell = 0$ diagonal.

Table 10

Raman Transition Moment Integral squared for a Particle on a Ring with a 5Å radius

m_ℓ/m_ℓ	0	1	2	3	4	5
0	0.25	0.00	0.06	0.00	0.00	0.00
1	0.00	0.25	0.00	0.06	0.00	0.00
2	0.06	0.00	0.25	0.00	0.06	0.00
3	0.00	0.06	0.00	0.25	0.00	0.06
4	0.00	0.00	0.06	0.00	0.25	0.00
5	0.00	0.00	0.00	0.06	0.00	0.25

Raman simulated spectrum

As seen in *Figure 6*, a Stokes scattered particle will lose energy, an anti-Stokes particle will gain energy, and the Rayleigh scattered particle will remain the same (eq 63-65). Therefore, the energy of a transition equates to the difference of the original energy and the scattered particle (eq 66-68).

$$E_{Rayleigh} = E_n \tag{63}$$

$$E_{Stokes} = E_n - E_{n \to n'} \tag{64}$$

$$E_{Anti-stokes} = E_n + E_{n\to n'} \quad (65)$$

$$E_{Rayleigh\ transition} = E_n - E_n = 0 \quad (66)$$

$$E_{Stokes\ transition} = E_n - (E_n - E_{n\to n'}) = E_{n\to n'} \quad (67)$$

$$E_{Anti-stokes} = E_n - (E_n + E_{n\to n'}) = -E_{n\to n'} \quad (68)$$

The Raman spectra intensity is classically plotted versus transition energy, so all the peaks are plotted based on their energy shift. By that, the Stokes and anti-Stokes scattering will shift positive and negative respectively from the unmoved Rayleigh scattering. The large Rayleigh peak is observed for all elastic scattering at energy zero (*Figure 25*). Since the Rayleigh scattering occurs at such a high incidence, the spectrum is scaled to better see the shifts (*Figure 26*).

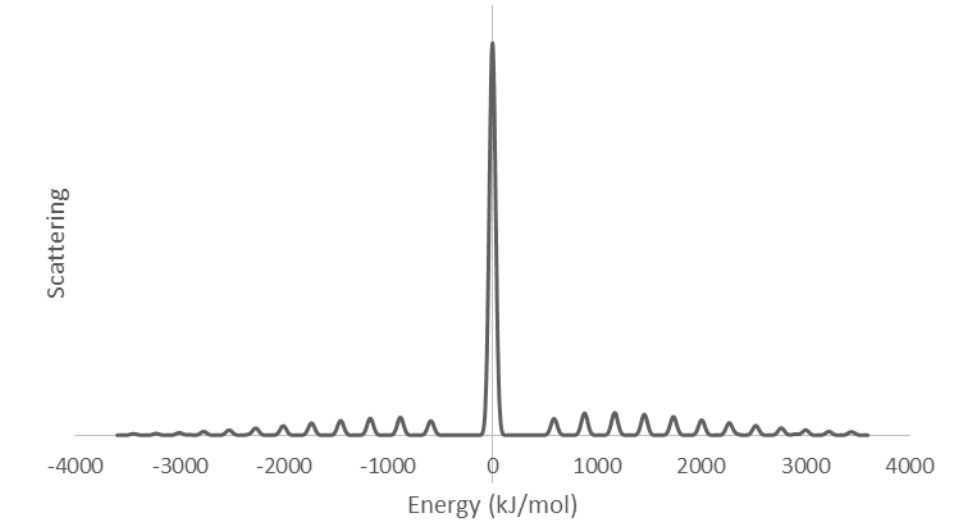

Figure 25. Simulated Raman spectrum for a 10Å particle in a box at 50000K.

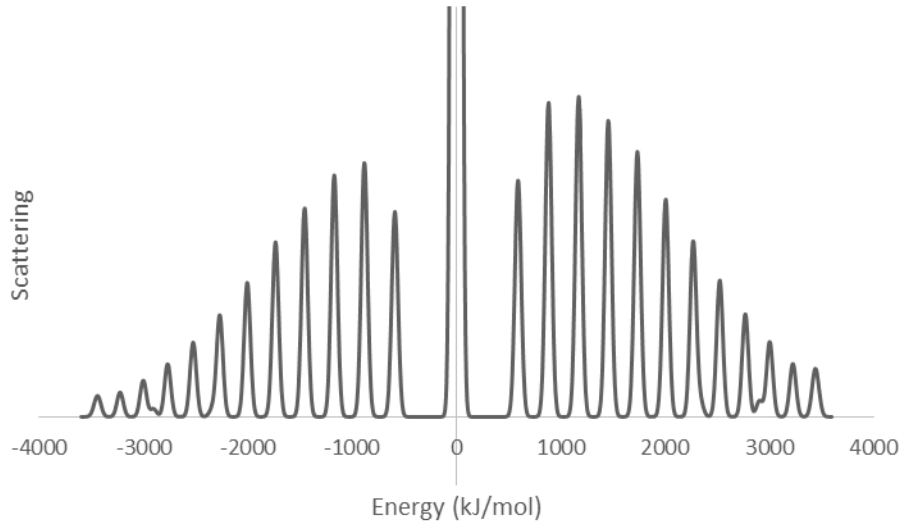

Figure 26. Scaled Raman spectrum for a 10Å particle in a box at 50000K.

The particle on a ring Raman spectrum was treated the same way as the particle in a box. The following figures show the normal and scaled spectrum based on the energy shift.

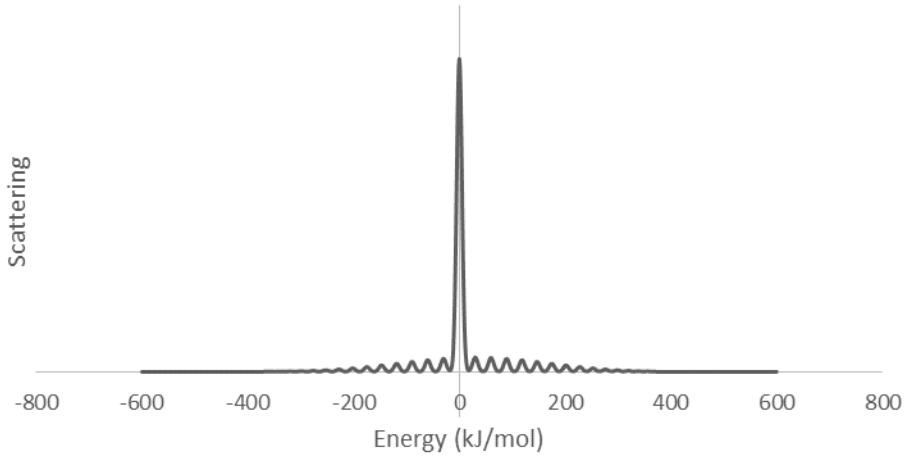

Figure 27. Raman spectrum for a particle on a ring with a 7Å radius.

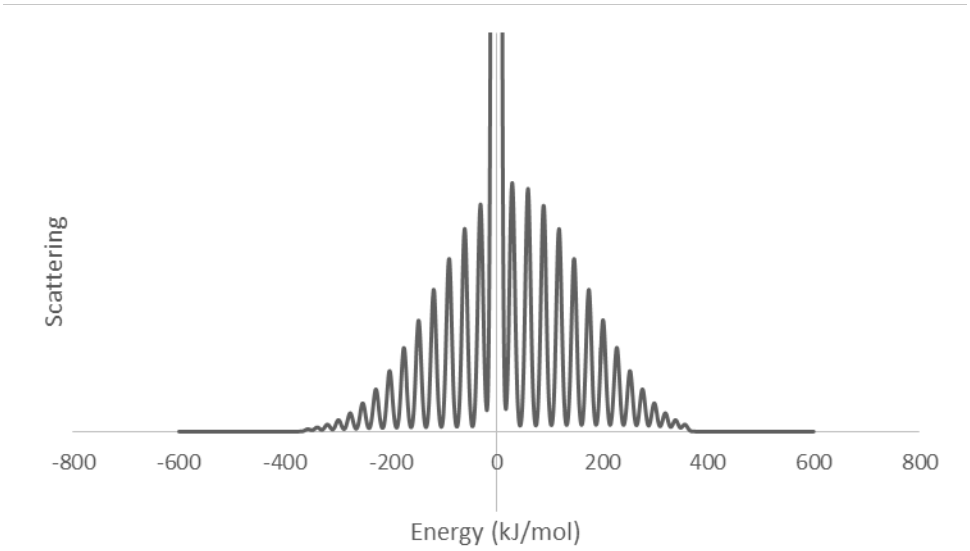

Figure 28. Scaled Raman spectrum for a particle on a ring with a 7Å radius.

CHAPTER IV

Symmetry Theory

An easy way to define selection rules, is to determine if the transition integral is a zero or non-zero value. Those transitions with an integral that equals zero are forbidden and those with nonzero integrals are allowed.[11]

Particle in a box Wave function symmetry

The particle in a box system is relatively easy to define. The shifted wave function allows an easy visual determination of odd or even symmetry with the axis splitting the middle of the wave function (*Figure 29-Figure 30*). Even functions will show a mirror image over the y-axis.

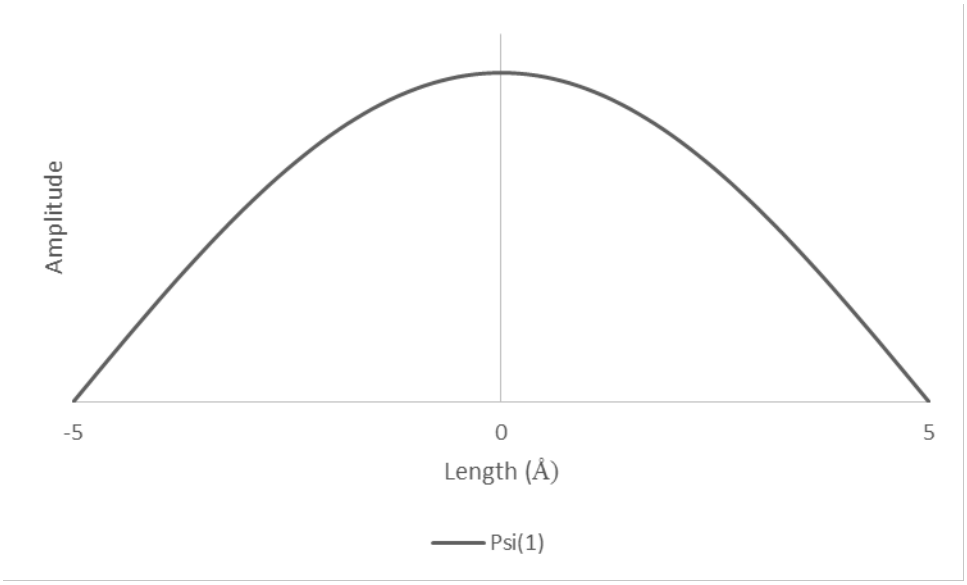

Figure 29. Even wave function at n=1 for particle in a 10Å box.

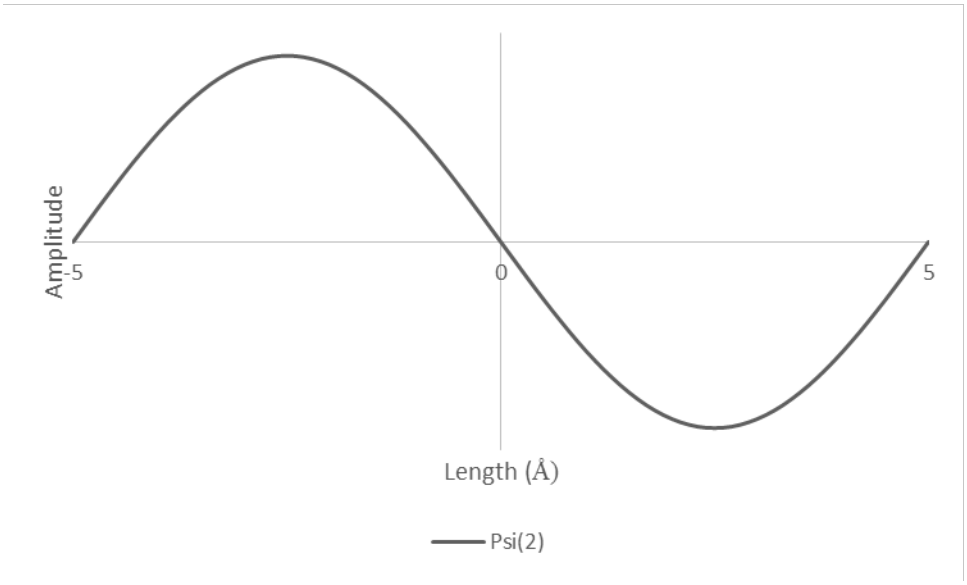

Figure 30. Odd wave function n=2 for particle in a 10Å box.

Integrand symmetry and Selection rule determination

Each wave function in the integrand is identified as having an odd or even symmetry based on the properties of even and odd functions. If f(x) equals f(-x), then f(x)is an even function, and if f(-x) equals –f(x), then f(x) is an odd function.[10] The electric dipole operator has a positive and negative region to produce the dipole therefore it is defined as an odd wave function. The product of each wave function in the transition and the dipole operator will yield the overall symmetry of the integrand (eq 69-70). Once integrated, an even wave function may produce a non-zero value possibly giving an allowed transition. The odd wave functions will cancel out the positive and negative parts and give a zero value producing a forbidden transition.

$$\langle Even|Odd|Even\rangle = \langle Even|Odd\rangle = \langle Odd\rangle = 0 \therefore Forbidden \quad (69)$$

$$\langle Odd|Odd|Even\rangle = \langle Odd|Odd\rangle = \langle Even\rangle \neq 0 \therefore Possibly\ Allowed \quad (70)$$

For the particle in a box, the wave function symmetry starts with even symmetry at *n*=1 then goes to odd symmetry at *n*=2, and this even then odd trend follows through all the quantum levels (eq 71-72). With this symmetry trend, the selection rules produced are Δn={±1,3,5…}.

$$\langle n|x|n+\Delta n_{even}\rangle = \langle Even|Odd|Even\rangle = \langle Odd\rangle = 0 \therefore Forbidden (71)$$

$$\langle n|x|n+\Delta n_{odd}\rangle = \langle Even|Odd|Odd\rangle = \langle Even\rangle \neq 0 \therefore Possibly\ Allowed (72)$$

For the transition moment integral, the electric dipole is a second order operator. This operator will be represented by two odd wave functions (eq 73-74). With the new operator the selection rules become Δn={±2,4,6…}.

$$\langle n|x|n+\Delta n_{even}\rangle = \langle Even|Odd, Odd|Even\rangle = \langle Even\rangle \neq 0 \therefore Possibly\ Allowed (73)$$

$$\langle n|x|n+\Delta n_{odd}\rangle = \langle Even|Odd, Odd|Odd\rangle = \langle Odd\rangle = 0 \therefore Forbidden (74)$$

Particle on a ring wave function symmetry

For the particle on a ring system with the circular nature of the coordinate system, the even or odd symmetry of the wave function is difficult to establish. The particle on a ring wave function has real and imaginary portions. Since Euler's relationship defines both portions as having the same symmetry merely shifted by $\frac{\pi}{2}$ from each other, the evaluation of only the real portion is enough to identify rotational wave function symmetry.

The symmetry of the ring-shaped coordinate system must be defined, and then the subsequent symmetry of each rotational wave function is derived from the character table of that point group (Table 11). Since the ring has the same symmetrical properties of a cylinder with an inversion center, the point group of $D_{\infty h}$ denotes its symmetry.[10] Another

view is through extrapolation from cyclopropane (D_{3h}) to benzene (D_{6h}) to a ring ($D_{\infty h}$) with infinite C_2 and σ_v giving the particle on a ring system a $D_{\infty h}$ symmetry.[10]

Table 11

$D_{\infty h}$ Character Table

$D_{\infty h}$	E	$2C_\infty^\varphi$	..	$\infty\sigma_v$	i	$2S_\infty^\varphi$	..	∞C_2	
$A_{1g}=\sum_g^+$	1	1		1	1	1		1	x^2+y^2,z^2
$A_{2g}=\sum_g^-$	1	1		-1	1	1		-1	R_z
$E_{1g}=\prod_g$	2	$2\cos(\phi)$		0	2	$-2\cos(\phi)$		0	(R_x,R_y) (xz,yz)
$E_{2g}=\Delta_g$	2	$2\cos(2\phi)$		0	2	$2\cos(2\phi)$		0	(x^2-y^2,xy)
E_{3g}	2	$2\cos(3\phi)$		0	2	$-2\cos(3\phi)$		0	
E_{4g}	2	$2\cos(4\phi)$		0	2	$2\cos(4\phi)$		0	
E_{ng}	2	$2\cos(n\phi)$		0	2	$(-1)^n\cos(n\phi)$		0	
$A_{1u}=\sum_u^+$	1	1		1	-1	-1		-1	z
$A_{2u}=\sum_u^-$	1	1		-1	-1	-1		1	
$E_{1u}=\prod_u$	2	$2\cos(\phi)$		0	-2	$2\cos(\phi)$		0	(x,y)
$E_{2u}=\Delta_u$	2	$2\cos(2\phi)$		0	-2	$2\cos(2\phi)$		0	
E_{3u}	2	$2\cos(3\phi)$		0	-2	$2\cos(3\phi)$		0	
E_{4u}	2	$2\cos(4\phi)$		0	-2	$2\cos(4\phi)$		0	
E_{nu}	2	$2\cos(n\phi)$		0	-2	$(-1)^{n+1}\cos(n\phi)$		0	

Each wave function is determined to be even (gerade) or odd (ungerade) by inspecting its behavior upon inversion through aerial observation of the positive and negative lobes on opposing sides of the ring (*Figure 31-Figure 32*).[13] Wave functions with lobes that are unchanged by inversion are gerade, *g*, while those which are inverted are ungerade, *u*. Further wave function classification is determined by recognizing that the characters under the rotational symmetry element ($2C_\infty^\phi$) are in fact the real portion of the particle on a ring wave function.[14] For example, the E_1 character $2\cos(\phi)$ is similar to the real part of the $m_\ell = \pm 1$ wave function, while the E_2 character $2\cos(2\phi)$ is similar to the real part of the $m_\ell = \pm 2$ wave function. The electric dipole μ of a charged particle is typically represented as the x-axis (μ_x). However, in the $D_{\infty h}$ character table, *x* and *y* are

inseparable and thus the dipole moment operator $\mu_{(x,y)}$ will have the E_{1u} irreducible representation. If this were a 3D system, μ_z (A_{1u}) would play a role, but with the electron confined to the *xy*-plane, a dipole along the z-axis is impossible.

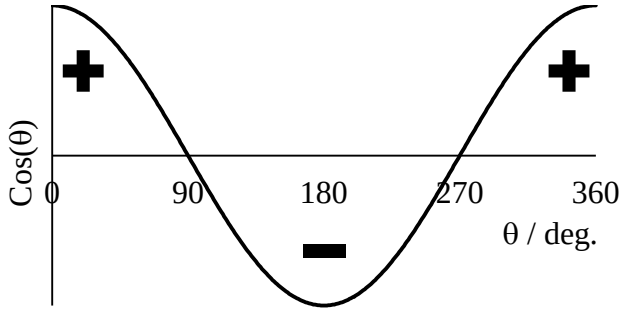

Figure 31. The rotational wave function $m_\ell = 1$ plotted from 0 to 2π (0^0 to 360°). Positive and negative lobes establish the positive and negative wedges in a top-down plot of the wave functions.

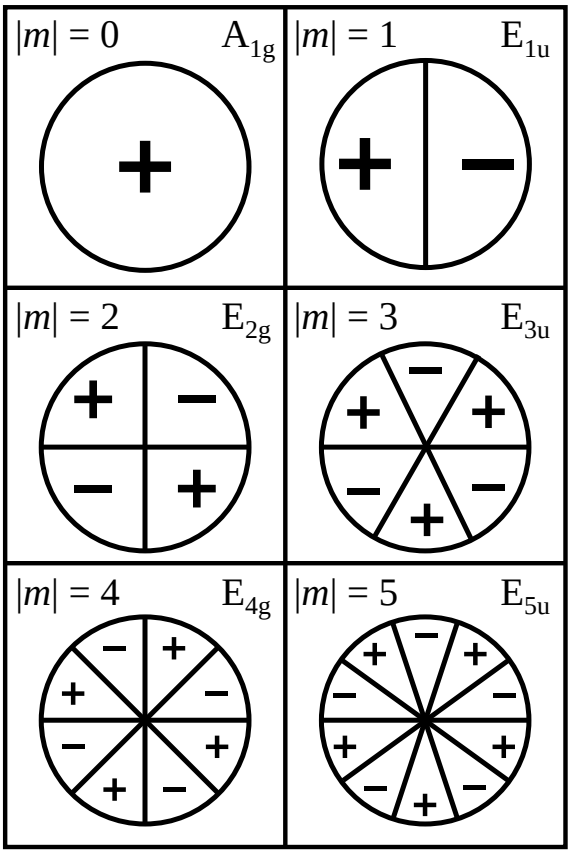

Figure 32. Top-down plot of the first six particle on a ring wave functions and their irreducible representations.

The product of the given irreducible representations in the transition will determine the overall symmetry of the transition dipole integrand. We found it necessary to expand the direct product tables to E_6 ($m_\ell = \pm 6$) to be sure of the selection rule trends. This expansion to produce Table 13 is illustrated in Table 12 which proves the authenticity of equation 75.

$$E_1 \otimes E_2 = E_1 \oplus E_3 \tag{75}$$

Table 12

An example showing the validity of equation 75

Representation	***E***	$2C_\infty^\phi$	$\infty\sigma_v$	***i***	$2S_\infty^\phi$	∞C_2
$\mathbf{E_{1g}}$	2	2cos(ϕ)	0	2	-2cos(ϕ)	0
$\mathbf{E_{2g}}$	2	2cos(2ϕ)	0	2	2cos(2ϕ)	0
$\mathbf{E_{3g}}$	2	2cos(3ϕ)	0	2	-2cos(3ϕ)	0
$\mathbf{E_1 \otimes E_2}$	4	2cos(ϕ) + 2cos(3ϕ)	0	4	-2cos(ϕ) – 2cos(3ϕ)	0
$\mathbf{E_1 \oplus E_3}$	4	2cos(ϕ) + 2cos(3ϕ)	0	4	-2cos(ϕ) – 2cos(3ϕ)	0

Table 13

$D_{\infty h}$ expanded Direct Product Table

$D_{\infty h}$	A_1	A_2	E_1	E_2	E_3	E_4	E_5	E_6
A_1	A_1	A_2	E_1	E_2	E_3	E_4	E_5	E_6
A_2		A_1	E_1	E_2	E_3	E_4	E_5	E_6
E_1			$A_1+A_2+E_2$	E_1+E_3	E_2+E_4	E_3+E_5	E_4+E_6	E_5+E_7
E_2				$A_1+A_2+E_4$	E_1+E_5	E_2+E_6	E_3+E_7	E_4+E_8
E_3					$A_1+A_2+E_6$	E_1+E_7	E_2+E_8	E_3+E_9
E_4						$A_1+A_2+E_8$	E_1+E_9	E_2+E_{10}
E_5							$A_1+A_2+E_{10}$	E_1+E_{11}
E_5								$A_1+A_2+E_{12}$

Integrand Symmetry and Selection Rule Determination

The symmetry of the integrand can be determined using the $D_{\infty h}$ direct product table. An allowed transition (i.e. nonzero value for the transition dipole moment integral) is obtained only if the symmetry of the integrand contains the totally symmetric irreducible representation A_{1g} in the $D_{\infty h}$ character table.[12] The following tables present the results for Δm_ℓ = { ±1, ±2, and ±3} which is enough to establish a trend that precludes any allowed higher Δm_ℓ transitions. The A_{1g} symmetry in the integrand in the direct product results in Table 14 yields an allowed transition, confirming the selection rule of $\Delta m_\ell = \pm 1$.

Table 14

Analysis showing that $\Delta m_\ell = \pm 1$ transitions are allowed by symmetry

Transition		***Symmetries***		***Result (all ≠ 0)***
$\langle 1 \vert \mu_{(x,y)} \vert 0 \rangle$	=	$\langle E_{1u} \vert E_{1u} \vert A_{1g} \rangle$	=	$\langle \boldsymbol{A_{1g}} \oplus A_{2g} \oplus E_{2g} \rangle$
$\langle m+1_{odd} \vert \mu_{(x,y)} \vert m_{even} \rangle$	=	$\langle E_{(m+1)u} \vert E_{1u} \vert E_{mg} \rangle$	=	$\langle \boldsymbol{A_{1g}} \oplus E_{2g} \oplus E_{2mg} \oplus A_{2g} \oplus E_{2(m+1)g} \rangle$
$\langle m+1_{even} \vert \mu_{(x,y)} \vert m_{odd} \rangle$	=	$\langle E_{(m+1)g} \vert E_{1u} \vert E_{mu} \rangle$	=	$\langle \boldsymbol{A_{1g}} \oplus E_{2g} \oplus E_{2mg} \oplus A_{2g} \oplus E_{2(m+1)g} \rangle$

The transitions with Δm_ℓ = {±2, ±4, …} are all forbidden due to the *g*-*u* product rules ($\Gamma_g \otimes \Gamma_g = \Gamma_g$; $\Gamma_u \otimes \Gamma_u = \Gamma_g$; $\Gamma_u \otimes \Gamma_g = \Gamma_u$). The resulting integrand will have *u* symmetry and cannot possibly contain A_{1g}.

An analysis of the results in Table 15 shows that the transitions from $m_\ell = 0$ to {±3, ±5, …} are forbidden because the result of these direct products will follow the E_1 row in Table 13 never yielding an integrand that contains A_{1g}.

Table 15

Analysis showing that $\Delta m_\ell = \pm 3$ transitions are forbidden by symmetry

Transition		***Symmetries***		***Result (all = 0)***
$\langle 3\|\mu_{(x,y)}\|0\rangle$	=	$\langle E_{3u}\|E_{1u}\|A_{1g}\rangle$	=	$\langle E_{2g}\oplus E_{4g}\rangle$
$\langle m_\ell + 3_{odd}\|\mu_{(x,y)}\|m_{\ell\,even}\rangle$	=	$\langle E_{(m_\ell+3)u}\|E_{1u}\|E_{m_\ell g}\rangle$	=	$\langle E_{(m_\ell+3)u}\|E_{(m_\ell+1)u}\oplus E_{(m_\ell-1)u}\rangle$
$\langle m_\ell + 3_{even}\|\mu_{(x,y)}\|m_{\ell\,odd}\rangle$	=	$\langle E_{(m_\ell+3)g}\|E_{1u}\|E_{m_\ell u}\rangle$	=	$\langle E_{(m_\ell+3)g}\|E_{(m_\ell+1)g}\oplus E_{(m_\ell-1)g}\rangle$

The $\Delta m_\ell = \pm 3$ transitions in Table 15 require some analysis of the trends seen in the direct product table (Table 13). They are forbidden because the only way to yield an A_{1g} irreducible representation would be for the direct product of $E_{1u}\otimes E_{m\ell}$ to yield an $E_{(m\ell+3)}$ irreducible representation. This is impossible because E_1 can only increase the subscript by one ($E_1\otimes E_{m\ell} = E_{(m\ell+1)}\oplus\ldots$). This same limitation will occur for all higher Δm_ℓ transitions, making $\Delta m_\ell = \pm 1$ the only allowed transition type in the particle on a ring system for direct absorption and emission spectroscopies.

The Rayleigh ($\Delta m_\ell = 0$) and Raman ($\Delta m_\ell = \pm 2$) scattering selection rules can be determined using this method. These scattering phenomena utilize the polarizability operator (α), which transforms as all the second-order terms (x^2+y^2, xz, etc) in the character table ($A_{1g}\oplus E_{1g}\oplus E_{2g}$).

$$I \propto \langle m_\ell'|\alpha|m_\ell\rangle^2 \tag{76}$$

$$I \propto \langle m_\ell'|A_{1g}\oplus E_{1g}\oplus E_{2g}|m_\ell\rangle^2 \tag{77}$$

The solution of equation 77 for the Rayleigh scattering selection rule ($\Delta m_\ell = 0$) is shown in Table 16. The first row yields an allowed transition because of the product of three A_{1g} irreducible representations. The second and third rows show that Rayleigh scattering is allowed for $m_\ell \neq 0$ because 1) the $E_{m\ell}$ on the right survives left-multiplication

by the A_{1g} portion of the polarizability operator and 2) the direct product of any irreducible representation with itself ($E_{m\ell} \otimes E_{m\ell}$) will contain A_{1g}.

Table 16

Analysis showing that Rayleigh scattering $\Delta m_\ell = 0$ is allowed by symmetry

Transition		***Symmetries***		***Result (all $\neq 0$)***
$\langle 0\|\alpha\|0\rangle$	=	0	=	$\langle \boldsymbol{A_{1g}} \oplus E_{1g} \oplus E_{2g} \rangle$
$\langle m_{\ell_{even}}\|\alpha\|m_{\ell_{even}}\rangle$	=	$\langle E_{m_\ell g}\|A_{1g} \oplus E_{1g} \oplus E_{2g}\|E_{m_\ell g}\rangle$	=	$\langle \boldsymbol{A_{1g}} \oplus \ldots \rangle$
$\langle m_{\ell_{odd}}\|\alpha\|m_{\ell_{odd}}\rangle$	=	$\langle E_{m_\ell u}\|A_{1g} \oplus E_{1g} \oplus E_{2g}\|E_{m_\ell u}\rangle$	=	$\langle \boldsymbol{A_{1g}} \oplus \ldots \rangle$

The allowed transitions for Raman scattering ($\Delta m_\ell = \pm 2$) are shown in Table 17. The first row in Table 17 yields an allowed transition because the E_{2g} in the polarizability operator survives multiplication on the right by A_{1g} and yields A_{1g} when left-multiplied by E_{2g}. The second and third rows in Table 17 show that Raman scattering is allowed for all $m_\ell \neq 0$ because $E_2 \otimes E_{m\ell} = E_{m-2} \oplus E_{m+2}$, and $E_{m\ell+2} \otimes E_{m\ell+2}$ will contain A_{1g}.

Table 17

Analysis showing that Raman scattering $\Delta m_\ell = \pm 2$ is allowed by symmetry

Transition		***Symmetries***		***Result (all $\neq 0$)***
$\langle 2\|\alpha\|0\rangle$	=	$\langle \boldsymbol{E_{2g}}\|A_{1g} \oplus E_{1g} \oplus \boldsymbol{E_{2g}}\|A_{1g}\rangle$	=	$\langle \boldsymbol{A_{1g}} \oplus \ldots \rangle$
$\langle m_\ell + 2_{even}\|\alpha\|m_{\ell_{even}}\rangle$	=	$\langle \boldsymbol{E}_{(m_\ell+2)g}\|A_{1g} \oplus E_{1g} \oplus \boldsymbol{E_{2g}}\|\boldsymbol{E}_{m_\ell g}\rangle$	=	$\langle \boldsymbol{A_{1g}} \oplus \ldots \rangle$
$\langle m_\ell + 2_{odd}\|\alpha\|m_{\ell_{odd}}\rangle$	=	$\langle \boldsymbol{E}_{(m_\ell+2)u}\|A_{1g} \oplus E_{1g} \oplus \boldsymbol{E_{2g}}\|\boldsymbol{E}_{m_\ell u}\rangle$	=	$\langle \boldsymbol{A_{1g}} \oplus \ldots \rangle$

The polarizability operator is even (gerade) while the electric dipole operator is odd (ungerade). Therefore, the $\Delta m_\ell = \{\pm 1, \pm 3, \ldots\}$ transitions fail the *g-u* symmetry requirement under the polarizability operator just as the $\Delta m_\ell = \{\pm 2, \pm 4, \ldots\}$ transitions fail the *g-u* symmetry requirement under the electric dipole operator.

Table 18 shows that $\Delta m = \pm 4$ transitions are forbidden even though they pass the *g-u* symmetry requirement. The only way to yield an A_{1g} irreducible representation would be for the direct product of $\alpha \otimes E_{m\ell}$ to yield an $E_{(m\ell+4)}$ irreducible representation. The polarizability tensor can only increase the subscript by two ($E_2 \otimes E_{m\ell} = E_{(m\ell+2)} \oplus \ldots$). This same limitation will occur for all higher Δm_ℓ transitions, making $\Delta m_\ell = \pm 2$ (+2 for Stokes shift; -2 for Anti-Stokes shift) the only allowed transition type in the particle on a ring system for Raman scattering.

Table 18

Analysis showing that Raman scattering with $\Delta m_\ell = \pm 4$ is forbidden by symmetry

Transition		***Symmetries***		***Result (all $\neq 0$)***
$\langle 4\|\alpha\|0\rangle$	=	$\langle E_{4g}\|A_{1g} \oplus E_{1g} \oplus E_{2g}\|A_{1g}\rangle$	=	$\langle E_{2g} \oplus E_{3g} \oplus E_{4g} \oplus E_{5g} \oplus E_{6g}\rangle$
$\langle m_\ell + 4_{even}\|\alpha\|m_{\ell_{even}}\rangle$	=	$\langle E_{(m_\ell+4)g}\|A_{1g} \oplus E_{1g} \oplus E_{2g}\|E_{m_\ell g}\rangle$	=	$\langle E_{(m_\ell+4)g}\|E_{(m_\ell+2)g} \oplus \cdots\rangle$
$\langle m_\ell + 4_{odd}\|\alpha\|m_{\ell_{odd}}\rangle$	=	$\langle E_{(m_\ell+4)u}\|A_{1g} \oplus E_{1g} \oplus E_{2g}\|E_{m_\ell u}\rangle$	=	$\langle E_{(m_\ell+4)u}\|E_{(m_\ell+2)u} \oplus \cdots\rangle$

CHAPTER V

Discussion

The three solutions for our particle in a box and particle on a ring system give a variety of information. All solutions have their pros and cons as well as giving different insights into quantum mechanics

Analytical Solution

The analytical solution produces equations showing dependence on the variables. Variables like length, mass, quantum level, and change in quantum level can be pinpointed as to their exact influence over energy and transitions. Variables in the numerator will have a direct relationship and those in the denominator will have an inverse relationship. The analytical relationship shows the step by step the mathematical proof for the integrals. This allows for a smaller scale very specific view of electronic behavior. This way one can follow a single wave function from energy to intensity. Though the analytical solution will give an exact answer and show the calculations step by step, the overall trends are hard to see. The big picture is tough to perceive when only one equation can be calculated at a time. Also without a visual representation of wave functions, conclusions as to why some integrals are produced is difficult. With the addition of the numerical view, wave function behavior is visually understood.

Numerical Solution

The numerical solution produces a dynamic spreadsheet showing the results of several wave functions. The dynamic ability of this set up allows instantaneous results from any variable change. The large range of wave functions allows for simultaneous comparison of different quantum levels and different quantum level transitions. This is

especially important for any visual learners to make the link from the abstract mathematics to the routine visual outputs seen with instruments. Though trends are easily seen in the numerical solution, the specific reasoning behind the trends still comes from the analytical solution. One can see energy is dependent on length, but only the analytical integral solution will show to what extent. All trends are deduced from the analytical calculation, but the numerical formulation gives the pictorial output of these trends.

Numerical Error

Table 4 and Table 5 show the increase in error between the analytical and numerical solution with an increase in quantum level. This shows why the numerical solution will not be as exact as the solution produced analytically. Since the spreadsheet adds the area under the curve with column blocks, as the curvature of the wave function increases it is harder for mere blocks to accurately calculate the curves (*Figure 33*). In the following figure, all of the white left under the curve are values missed by the numerical solution giving the negative bias. With the increase in curvature for higher quantum numbers, this white space will increase therefore giving the increase in error.

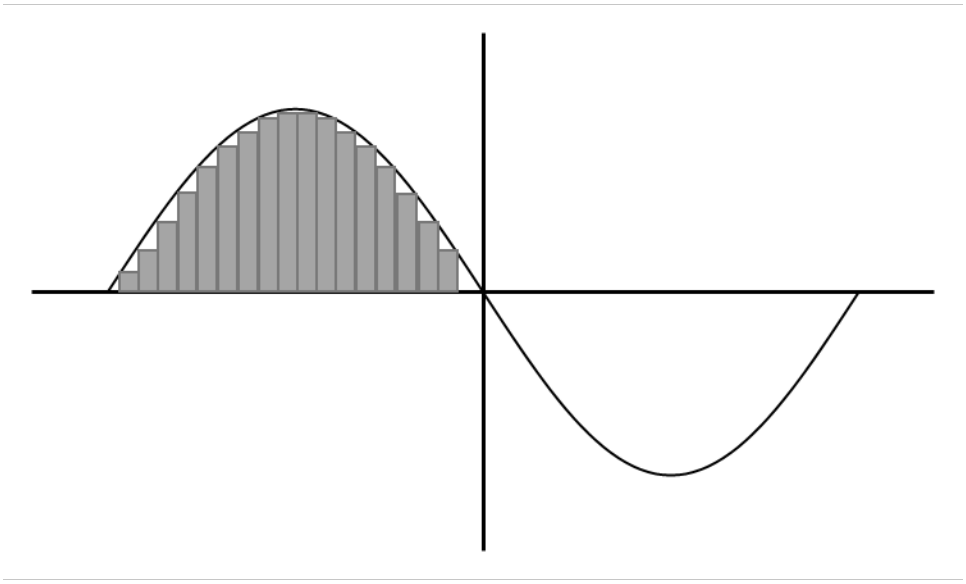

Figure 33. Depiction of numerical integration.

Symmetry Solution

The symmetry based solution shows a quick way to the selection rules. Symmetry is the simplest of all the solutions and therefore is the most likely to be understood. This way will give whether the transition integral is a zero or non-zero value therefore producing selection rules, but there will be no comment on the degree to which any of these transitions will occur. Symmetry allows one to simply look at the wave functions in a transition and determine if it is allowed or not allowed. The fact that symmetry can govern the selection rules shows the importance of symmetry even in molecular behavior.

Wave function behavior

The numerical solution allowed for the depiction of wave function behavior. For particle in a box, one can see in *Figure 7* the wave functions approach zero at the boundary conditions of the box. The rise in quantum number gives an increased in wave function curvature and in the number of lobes and nodes. The dynamic ability of the spreadsheet shows the amplitude differences with the change in box length, a trend not ascertained from the analytical formulation. As the length of the box decreases from *Figure 7* to *Figure 8*, the amplitude of the wave function increases.

Using the same numerical solution, the particle on a ring wave functions can be inspected. With a decrease in radius from *Figure 9* to *Figure 10*, the amplitude does not change. Even though the amplitude is unchanged, the curvature visibly increases since the same wave function is being squeezed into a smaller circumference.

Energy Equation

In the quantized energy equation for particle in a box, mass and length are both in the denominator (eq 27.3). Therefore, the energy varies inversely with mass and the square of the length. At a smaller mass and length, the quantization is clearly seen since energy and spacing between levels is large. As the mass and length become greater, these discrete levels will become less noticeable since energy and spacing between levels become small. The larger scale will begin to mimic energy seen in classical chemistry. Numerically, the graphed wave function shows an increase in amplitude when the length of the box decreases (*Figure 8*). This shows the increase of energy with a decrease in box length. The numerator of this equation includes the squared quantum number therefore making energy vary directly with the squared quantum number. As the quantum levels rise so will the energy. The graphed wave functions show a higher frequency for the wave function with increase quantum levels. These increased level wave functions have more lobes and nodes thus displaying the higher energy.

Since particle in a box quantum levels start at n=1, electronic energy can never be zero. This creates the idea that zero point energy, the lowest possible energy a system may have, cannot be zero.[11] Conversely with the particle on a ring, rotational levels can have a quantum state of zero. This allows rotational energy to be zero and therefore no rotational particle movement.

Just as with the particle in a box, the particle on a ring energy equation shows a direct relationship with the quantum level and an inverse relationship with both the particle mass and the ring radius (eq 28.3). The only difference comes from the inclusion of a pi squared constant in the denominator coming from the particle on a ring wave

function. The wave functions again show the increase in nodes with increased quantum number, but they show no change in amplitude with the change in radius. Instead, the increase in curvature illustrates the increase in energy with a decrease in ring radius.

Boltzmann Distribution

Numerically, the Boltzmann distribution plays a large role in giving a more realistic transition intensity. This distribution regulates the population of a quantum level. Without a particle populating the level, even if the transition is allowed by the selection rules, the transition will not be observed. An increase in degeneracy will increase the probability of a level being populated. Specifically for particle in a ring, this will increase the probability of an electron being in the higher quantum levels. Conversely, increasing energy will drop the Boltzmann distribution which then makes those higher quantum levels hard to populate. Though, increasing the temperature will again increase the probability of an electron populating high energy levels.

Transition Dipole Moment Integral

In the transition dipole moment, the electric dipole interacts with the wave function. *Figure 17* and *Figure 18* are the wave functions perturbed by the electric dipole, and show a change of symmetry in the wave functions. This change of symmetry, seen in the symmetry solution, will cause previously orthogonal wave functions to now interact (eq 69-70). The analytical integral from particle in a box gives insight into the system variable dependence of transitional intensity for electronic spectra (eq 33). With length being in the numerator, the transition dipole moment integral intensity is directly related, so as the length increases so will the intensity of transitions. Since quantum number and change in quantum number are in the denominator, the transition dipole moment integral

would be thought to be inversely related. In actuality, since the quantum number is found only in the smaller opposing argument, it has a conflicting effect and switches to a direct relationship with the intensity. This means as the quantum level increases, so will the intensity of the transition. The change in quantum number is found in both the positive and negative argument's denominators, but it plays a bigger role in the numerically larger argument, therefore it will have an inverse relationship with intensity. Meaning, as the quantum change in the transition increases, the intensity of this transition will decrease. In Table 7 shows the same particle in a smaller 7Å box.

Table 6, the numerical transition dipole moment integral shows a agreeing decrease in intensity as the transition (Δn) increases. The intensity visibly increases as the energy levels increase. Though, one must remember as the energy increases, the Boltzmann distribution will decrease.

The transition dipole moment integral for particle on a ring shows a constant transition intensity (eq 38.3). Since the transition dipole integral is a constant, any changes in the ring or quantum number will not change the intensity value from the transition dipole approximation. Without a visualization of these wave functions it is hard to determine why this is happening. Once taking into account the constant wave function amplitude, this constant is plausible. This constant amplitude lends to the constant interaction in transition integral (*Figure 9-Figure 10*).

Transition Moment Integral

For particle in a box, the same intensity trends apply to Raman transitions as those in the direct transitions (eq 41). This integral is almost identical to the one calculated from the transition dipole moment integral. One can conclude that even though the

selection rules have changes, the variables that determine the degree of the intensity remain constant regardless of the electric operator. Rayleigh scattering does have a slightly different integral output, but will follow the same trends with length in the numerator and the quantum state in the negative argument's denominator (eq 42.3). Once numerically calculated, the transition dipole output clearly shows Rayleigh scattering to have a higher incidence of occurring a trend not determined in the analytical solution (Table 9).

For particle on a ring, again all of these intensity values for the particle on a ring are constants, and no change to the system will alter the intensity (eq 46.3 & 47.3). The Rayleigh scattering gives a non-zero value with a doubled intensity compared to the allowed Raman scattering. This intensity difference is plausible since same quantum level wave functions overlap even without the electric dipole as proven with the normalization, and wave functions of different quantum levels are completely independent until the interaction with the electric dipole as proven with orthogonality.

Theoretical Spectrum

The various theoretical spectra created in the numerical solution give a chance to visually see the quantum effects applied to common instrumental data. In the individual transitions for the particle in a box absorption spectrum seen in *Figure 20*, the largest absorbance does not come from the highest intensity peaks. In this case, a wavelength with many overlapping smaller peaks will sum to a large peak seen in the theoretical spectrum. This shows the many transitions that go into a single absorption spectrum.

Figure 23 shows the direct absorption spectrum for particle on a ring. The first fundamental peak is the transition from $0 \rightarrow 1$. The particle on a ring is doubly degenerate,

so m_ℓ =0 can transition to m_ℓ=1 or m_ℓ =-1. The m_ℓ =1 and m_ℓ =-1levels have the same energy, so the 0→1 peak will be double in intensity. All transitions above m_ℓ =0 are doubly degenerate, so the intensity duplication is seen through-out the entire spectrum. *Figure 22* is the transition peak versus the actual absorbance spectra which shows this duplication of intensity. Since the transition dipole moment integral is a constant for particle on a ring the slowly decreasing intensity is solely based on the Boltzmann distribution. As the energy of the levels increase, the Boltzmann distribution will decrease and the intensity will slowly drop off.

In the scaled Raman spectrum for particle on a ring in *Figure 28*, the three types of scattering are clearly represented. Rayleigh scattering is seen at energy zero. Since this can occur at multiple starting energy levels, a huge peak occurs at energy zero. The scaled Raman allows for the resolution of the $\Delta m_\ell \pm 2$ peaks. To the right are the Δm_ℓ =2 transitions with a constant increasing transition energy. To the left are the Δm_ℓ =-2 transitions with a constant decreasing transition energy. The first occurring peak to the right for the 0→2 transition shows a slightly higher intensity than the first occurring peak to the left for the 2→0 transition. Though these are the same transition just in different directions, the Boltzmann distribution is larger at the m_ℓ =0 ground state and therefore will give a higher intensity peak for the Stokes shifted peak. If graphed in wavenumber, the spectrum will be plotted as a wavenumber shift. This is representative of the shift away from the Rayleigh scattering that occurs at the incident light. Since this is a simulated spectrum and we do not have an incident light wavenumber, our plots remain as energy.

The Raman spectrum for particle in a box shows the same trends seen in the particle on a ring Raman spectrum (*Figure 26*). All the Stokes transitions have a higher intensity as the transition occurs from a quantum level with a higher Boltzmann distribution. This spectrum does have a few differences. Further out into the shifts there is some overlapping of peaks not seen it the particle on a ring Raman. The particle in a box selection rules allows many more transitions such as the Δn of 4 or 6. Though these transitions do not always occur, our spectrum was simulated at a high enough temperature to see some starting at the shift of about 3000 kJ/mol. Another difference seen is the large gap between the Rayleigh peaks and the Stokes and anti-Stokes peaks. For the particle in a box there is no n=0 quantum level, so the first transition will not originate from 0 kJ/mol as seen for the particle on ring. Therefore, there is a slightly gap from the Δ0 kJ/mol transition energy Rayleigh peak to the first Stokes and anti-Stokes peak.

Application

Linking particle in a box and particle on a ring to larger systems is a good way to show how these simple systems are the basis of many larger systems. Pi electrons in a conjugated molecule are a good example of an applicable use for the particle in a box. Just like the particle in a box, the conjugated pi-system is singly degenerate. This allows the calculation of the length of the pi bonded network found by the particle in a box by using the HOMO-LUMO transition wave length.[15] The experimental network length is comparable to theoretical network length calculated using the particle in a box system.[15] Though this experiment only determines values from the wave length axis, one can draw conclusions on the intensity of transitions. Since our theoretical intensity is only a

proportional intensity, we cannot calculate a real world intensity but rather trends in changes. The seen spectrum shows an increase in intensity with the increase in network length. This relative trend agrees with the conclusion made that an increased box length will decrease the intensity.

Quantum dots are another example of an applicable use for the particle in a box. In a quantum dot, light will promote electrons from the valence band into the conduction band.[16] The valence band and conduction band are considered discrete energy levels, and are dependent on the size of the quantum dot. Just as demonstrated with particle in a box, the emission wavelength increases as the diameter of the quantum dot increases.[11] Also evident in the experimental spectrum is the increase in intensity with the increase in emission wavelength.[16] This observation again confirms the trend that a larger length box will produced a larger intensity peak.

Cyclic polyynes are an applicable example for particle on a ring. This molecule has alternating single and triple bonds. The particle on a ring can model the pi electrons on the molecular ring.[17] The pi electrons out of the plane can lead to the theoretical calculation of the absorption wave length. This will demonstrate rotation in two dimensions seen with particle on a ring. This experiment shows the calculated transition wavelength with the energy equation comparable to the experimental wavelength.

CHAPTER VI

Conclusion

Completing all three solution techniques gives a comprehensive understanding of electron behavior in electronic and rotational transitions. Through these three solutions, the particle in a box mimicked the electronic behavior and the particle on a ring mimicked the rotational behavior of an electron.

The calculation of the Schrödinger equation for each system ascertained their respective energy equations. These equations gave the energy for discrete energy levels for each quantum state. This energy could be used to determine transition energy and transition wavelength between any quantum level.

The particle in a box concluded selection rules for electronic direct absorption and emission to be $\Delta n=\{\pm1,3,5\ldots\}$ and for Raman scattering to be $\Delta n=\{\pm2,4,6\ldots\}$. The particle on a ring concluded selection rules for rotational direct absorption and emission to be $\Delta m_\ell = \pm1$ and for Raman scattering to be $\Delta m_\ell = \pm2$. These were all determined by solving the transition dipole moment integral and transition moment integral. The square of these integrals combined with the Boltzmann distribution gave the proportional intensity of each allowed transition.

This information was combined to create simulated spectra. Created was an absorption spectrum, a rotational absorption spectrum, a Raman spectrum, and a rotational Raman spectrum. These simulated spectra built from simple systems allowed for the breakdown of the electronic behavior that goes into producing instrumental data.

REFERENCES

(1) Amore, P.; Fernández, F. M. On the Symmetry of Three Identical Interacting Particles in a One-Dimensional Box. *Ann. Phys. (N. Y).* **2015**, *362*, 118–129.

(2) Al-Hashimi, M. H.; Wiese, U. J. From a Particle in a Box to the Uncertainty Relation in a Quantum Dot and to Reflecting Walls for Relativistic Fermions. *Ann. Phys. (N. Y).* **2012**, *327* (1), 1–28.

(3) Hamidi, O.; Dehghan, H. Klein-Gordon Particle in a One-Dimensional Box with a Moving Wall. *Reports Math. Phys.* **2014**, *73* (1), 11–16.

(4) Menon, G.; Belyi, S. Dirac Particle in a Box, and Relativistic Quantum Zeno Dynamics. *Phys. Lett. Sect. A Gen. At. Solid State Phys.* **2004**, *330*, 33–40.

(5) Bakke, K.; Furtado, C. On the Confinement of a Dirac Particle to a Two-Dimensional Ring. *Phys. Lett. Sect. A Gen. At. Solid State Phys.* **2012**, *376* (15), 1269–1273.

(6) Vincent, A. An Alternative Derivation of the Energy Levels of the “Particle on a Ring” System. *J. Chem. Educ.* **1996**, *73* (10), 1001–1003.

(7) Chattaraj, P. K.; Sannigrahi, A. B. A Simple Group-Theoretical Derivation of the Selection Rules for Rotational Transitions. *J.Chem.Educ.* **1990**, *67* (8), 653–655.

(8) Das, R.; Sannigrahi, A. B. Simple Derivation of Some Basic Selection Rules. *J. Chem. Educ.* **1980**, *57* (3), 786–788.

(9) Yamasaki, K. Simple Way of Labeling Rotational Levels. *J. Chem. Educ.* **1966**, *68* (7), 574–575.

(10) Atkins, P. *Molecular Quantum Mechanics*, 2nd ed.; Butler & Tanner Ltd: Somerset, 1983.

(11) Engel, T.; Reid, P. *Physical Chemistry*, 3rd ed.; Pearson: New York, 2013.

(12) Harris, D. C.; Bertolucci, M. D. *Symmetry and Spectroscopy*; Dover Publications Inc.: Mineola, NY, 1978.

(13) Cotton, F. A. *Chemical Applications of Group Theory*, 3rd ed.; John Wiley & Sons Inc.: New York, 1990.

(14) Levine, I. N. *Quantum Chemistry*, 5th ed.; Prentice-Hall Inc.: Uppeer Saddle River, 2000.

(15) Anderson, B. D. Alternative Compounds for the Particle in a Box Experiment. *J. Chem. Educ.* **1997**, *74* (8), 985.

(16) Rice, C. V.; Giffin, G. a. Quantum Dots in a Polymer Composite: A Convenient Particle-in-a-Box Laboratory Experiment. *J. Chem. Educ.* **2008**, *85* (6), 842.

(17) Anderson, B. D. Cyclic Polyynes as Examples of the Quantum Mechanical Particle on a Ring. *J. Chem. Educ.* **2012**, *89* (6), 724–727.

APPENDIX A

Particle in a box solution for normalization constant.

$$\langle \psi_n | \psi_m \rangle = 1 \quad when\ n = m$$

$$\int_{-\frac{L}{2}}^{\frac{L}{2}} N \sin\left(\frac{n\pi x}{L} + \frac{n\pi}{2}\right) N \sin\left(\frac{n\pi x}{L} + \frac{n\pi}{2}\right) dx = 1$$

$$N^2 \int_{-\frac{L}{2}}^{\frac{L}{2}} \sin^2\left(\frac{n\pi x}{L} + \frac{n\pi}{2}\right) dx$$

$$N^2 \int_{-\frac{L}{2}}^{\frac{L}{2}} \frac{1}{2} - \frac{1}{2}\cos\left(\frac{2n\pi x}{L} + n\pi\right) dx$$

$$\frac{N^2}{2} \int_{-\frac{L}{2}}^{\frac{L}{2}} dx - \frac{N^2}{2} \int_{-\frac{L}{2}}^{\frac{L}{2}} \cos\left(\frac{2n\pi x}{L} + n\pi\right) dx$$

$$\frac{N^2}{2} x - \frac{N^2 L}{4n\pi} \sin\left(\frac{2n\pi x}{L} + n\pi\right)\Big|_{-\frac{L}{2}}^{\frac{L}{2}}$$

$$\left[\left(\frac{N^2 L}{4}\right) - \left(-\frac{N^2 L}{4}\right)\right] - 0 = 1$$

$$N = \sqrt{\frac{2}{L}}$$

Particle in a box solution for normalization.

$$\langle \psi_n | \psi_m \rangle = 1 \quad when\ n = m$$

$$\int_{-\frac{L}{2}}^{\frac{L}{2}} \sqrt{\frac{2}{L}} \sin\left(\frac{n\pi x}{L} + \frac{n\pi}{2}\right) \sqrt{\frac{2}{L}} \sin\left(\frac{n\pi x}{L} + \frac{n\pi}{2}\right) dx$$

$$\frac{2}{L}\int_{-\frac{L}{2}}^{\frac{L}{2}} \sin^2\left(\frac{n\pi x}{L}+\frac{n\pi}{2}\right)dx$$

$$\frac{2}{L}\int_{-\frac{L}{2}}^{\frac{L}{2}} \frac{1}{2}-\frac{1}{2}\cos\left(\frac{2n\pi x}{L}+n\pi\right)dx$$

$$\frac{1}{L}\int_{-\frac{L}{2}}^{\frac{L}{2}} dx-\frac{1}{L}\int_{-\frac{L}{2}}^{\frac{L}{2}} \cos\left(\frac{2n\pi x}{L}+n\pi\right)dx$$

$$\frac{x}{L}-\frac{1}{2n\pi}\sin\left(\frac{2n\pi x}{L}+n\pi\right)\Big|_{-\frac{L}{2}}^{\frac{L}{2}}$$

$$\left[\left(\frac{1}{2}\right)-\left(-\frac{1}{2}\right)\right]-0=1$$

Particle on a ring solution for normalization constant.

$$\langle\psi_{m_\ell}|\psi_{m'_\ell}\rangle = 1 \quad when\ m_\ell = m'_\ell$$

$$\int_{-\pi}^{\pi} Ne^{-im_\ell\phi}\, Ne^{im_\ell\phi} d\phi = 1$$

$$N^2\int_{-\pi}^{\pi} e^0\, d\phi = 1$$

$$N^2\phi|_{-\pi}^{\pi} = 1$$

$$N^2\pi-(-N^2\pi)=1$$

$$N=\sqrt{\frac{1}{2\pi}}$$

Particle on a ring solution for normalization.

$$\langle \psi_{m_\ell} | \psi_{m'_\ell} \rangle = 1 \quad when\ m_\ell = m'_\ell$$

$$\int_{-\pi}^{\pi} \sqrt{\frac{1}{2\pi}} e^{-im_\ell \phi} \sqrt{\frac{1}{2\pi}} e^{im_\ell \phi} d\phi$$

$$\frac{1}{2\pi} \int_{-\pi}^{\pi} e^0 \, d\phi$$

$$\frac{\phi}{2\pi} \Big|_{-\pi}^{\pi}$$

$$\frac{\pi}{2\pi} - \frac{-\pi}{2\pi} = 1$$

APPENDIX B

Derivation for orthogonality of particle in a box wave function.

$$\langle \psi_n | \psi_m \rangle = 0 \quad when\ n \neq m$$

$$\int_{-\frac{L}{2}}^{\frac{L}{2}} \sqrt{\frac{2}{L}} \sin\left(\frac{n\pi x}{L} + \frac{n\pi}{2}\right) \sqrt{\frac{2}{L}} \sin\left(\frac{m\pi x}{L} + \frac{m\pi}{2}\right) dx$$

$$\frac{2}{L} \int_{-\frac{L}{2}}^{\frac{L}{2}} \sin\left(\frac{n\pi x}{L} + \frac{n\pi}{2}\right) \sin\left(\frac{m\pi x}{L} + \frac{m\pi}{2}\right) dx$$

$$\frac{1}{L} \int_{-\frac{L}{2}}^{\frac{L}{2}} \cos\left(\frac{n\pi x}{L} + \frac{n\pi}{2} - \frac{m\pi x}{L} - \frac{m\pi}{2}\right) - \cos\left(\frac{n\pi x}{L} + \frac{n\pi}{2} + \frac{m\pi x}{L} + \frac{m\pi}{2}\right) dx$$

$$\frac{1}{L} \int_{-\frac{L}{2}}^{\frac{L}{2}} \cos\left(\frac{n\pi x}{L} + \frac{n\pi}{2} - \frac{m\pi x}{L} - \frac{m\pi}{2}\right) dx - \frac{1}{L} \int_{-\frac{L}{2}}^{\frac{L}{2}} \cos\left(\frac{n\pi x}{L} + \frac{n\pi}{2} + \frac{m\pi x}{L} + \frac{m\pi}{2}\right) dx$$

$$\frac{1}{n\pi - m\pi} \sin\left(\frac{n\pi x}{L} + \frac{n\pi}{2} - \frac{m\pi x}{L} - \frac{m\pi}{2}\right) - \frac{1}{n\pi + m\pi} \sin\left(\frac{n\pi x}{L} + \frac{n\pi}{2} + \frac{m\pi x}{L} + \frac{m\pi}{2}\right) \Bigg|_{-\frac{L}{2}}^{\frac{L}{2}}$$

$$0 - 0 = 0$$

Derivation for orthogonality of particle on a ring wave function.

$$\langle \psi_{m_\ell} | \psi_{m'_\ell} \rangle = 0 \quad when\ m_\ell \neq m'_\ell$$

$$\int_{-\pi}^{\pi} \sqrt{\frac{1}{2\pi}} e^{-im_\ell \phi} \sqrt{\frac{1}{2\pi}} e^{im'_\ell \phi} d\phi$$

$$\frac{1}{2\pi} \int_{-\pi}^{\pi} e^{i\phi(-m_\ell + m'_\ell)}\, d\phi$$

$$\frac{1}{2\pi} \frac{1}{i(-m_\ell + m'_\ell)} e^{i\phi(-m_\ell + m'_\ell)} \Big|_{-\pi}^{\pi}$$

$$\frac{1}{2\pi}\frac{1}{i(-m_\ell + m'_\ell)} e^{i\pi(-m_\ell + m'_\ell)} - \frac{1}{2\pi}\frac{1}{i(-m_\ell + m'_\ell)} e^{i-\pi(-m_\ell + m'_\ell)}$$

$$\frac{1}{2\pi}\frac{1}{i(-m_\ell + m'_\ell)} - \frac{1}{2\pi}\frac{1}{i(-m_\ell + m'_\ell)} = 0$$

APPENDIX C

Particle in a box full derivation of quantized energy equation.

$$\hat{\mathrm{H}}\psi_n = E_n\psi_n$$

$$\left(-\frac{\hbar^2}{2m}\right)\frac{\partial^2}{\partial x^2}\sqrt{\frac{2}{L}}\sin\left(\frac{n\pi x}{L}+\frac{n\pi}{2}\right) = E_n\sqrt{\frac{2}{L}}\sin\left(\frac{n\pi x}{L}+\frac{n\pi}{2}\right)$$

$$\left(-\frac{\hbar^2}{2m}\right)\left(\frac{n\pi}{L}\right)\frac{\partial}{\partial x}\sqrt{\frac{2}{L}}\cos\left(\frac{n\pi x}{L}+\frac{n\pi}{2}\right) = E_n\sqrt{\frac{2}{L}}\sin\left(\frac{n\pi x}{L}+\frac{n\pi}{2}\right)$$

$$\left(\frac{\hbar^2}{2m}\right)\left(\frac{n\pi}{L}\right)^2\sqrt{\frac{2}{L}}\sin\left(\frac{n\pi x}{L}+\frac{n\pi}{2}\right) = E_n\sqrt{\frac{2}{L}}\sin\left(\frac{n\pi x}{L}+\frac{n\pi}{2}\right)$$

$$\left(\frac{\hbar^2}{2m}\right)\left(\frac{n\pi}{L}\right)^2 = E_n$$

$$\left(\frac{\hbar^2 n^2\pi^2}{2mL^2}\right) = E_n \qquad \left(\hbar = \frac{h}{2\pi}\right)$$

$$E_n = \left(\frac{h^2 n^2}{8mL^2}\right)$$

Particle on a ring full derivation of quantized energy equation.

$$\hat{\mathrm{H}}\psi_{m_\ell} = E_{m_\ell}\psi_{m_\ell}$$

$$\left(-\frac{\hbar^2}{2mr^2}\right)\frac{\partial^2}{\partial\phi^2}\sqrt{\frac{1}{2\pi}}e^{-im_\ell\phi} = E_{m_\ell}\sqrt{\frac{1}{2\pi}}e^{-im_\ell\phi}$$

$$\left(-\frac{\hbar^2}{2mr^2}\right)(-m_\ell)\frac{\partial}{\partial x}\sqrt{\frac{1}{2\pi}}e^{-im_\ell\phi} = E_{m_\ell}\sqrt{\frac{1}{2\pi}}e^{-im_\ell\phi}$$

$$\left(-\frac{\hbar^2}{2mr^2}\right)(-m_\ell{}^2)\sqrt{\frac{1}{2\pi}}e^{-im_\ell\phi} = E_{m_\ell}\sqrt{\frac{1}{2\pi}}e^{-im_\ell\phi}$$

$$\left(\frac{m_l{}^2\hbar^2}{2mr^2}\right)\sqrt{\frac{1}{2\pi}}e^{-im_\ell\phi} = E_{m_\ell}\sqrt{\frac{1}{2\pi}}e^{-im_\ell\phi}$$

$$\left(\frac{m_l{}^2\hbar^2}{2mr^2}\right) = E_{m_\ell} \qquad \left(\hbar = \frac{h}{2\pi}\right)$$

$$E_{m_\ell} = \left(\frac{m_l{}^2\mathrm{h}^2}{8m\pi^2r^2}\right)$$

APPENDIX D

Transition Dipole Moment Integral for Particle in a box with an odd Δn

$$\langle \psi_n | x | \psi_{n+\Delta n} \rangle$$

$$\int_{-\frac{L}{2}}^{\frac{L}{2}} x sin\left(\frac{n\pi x}{L} + \frac{n\pi}{2}\right) sin\left(\frac{(n+\Delta n)\pi x}{L} + \frac{(n+\Delta n)\pi}{2}\right) dx$$

$$\int_{-\frac{L}{2}}^{\frac{L}{2}} x sin\left(\frac{n\pi x}{L} + \frac{n\pi}{2}\right) \sin\left(\frac{n\pi x}{L} + \frac{\Delta n\pi x}{L} + \frac{n\pi}{2} + \frac{\Delta n\pi}{2}\right) dx$$

$$\frac{2}{L}\int_{-\frac{L}{2}}^{\frac{L}{2}} \frac{x}{2}\left(cos\left(\frac{n\pi x}{L} + \frac{n\pi}{2} - \frac{n\pi x + \Delta n\pi x}{L} - \frac{n\pi + \Delta n\pi}{2}\right) - cos\left(\frac{n\pi x}{L} + \frac{n\pi}{2} + \frac{n\pi x + \Delta n\pi x}{L} + \frac{n\pi + \Delta n\pi}{2}\right)\right) dx$$

$$\frac{2}{L}\int_{-\frac{L}{2}}^{\frac{L}{2}} \frac{x}{2}\left(cos\left(-\frac{\Delta n\pi x}{L} - \frac{\Delta n\pi}{2}\right) - cos\left(\frac{2n\pi x + \Delta n\pi x}{L} + \frac{2n\pi + \Delta n\pi}{2}\right)\right) dx$$

$$\frac{1}{L}\int_{-\frac{L}{2}}^{\frac{L}{2}} xcos\left(-\frac{\Delta n\pi x}{L} - \frac{\Delta n\pi}{2}\right) dx - \frac{1}{L}\int_{-\frac{L}{2}}^{\frac{L}{2}} xcos\left(\frac{2n\pi x + \Delta n\pi x}{L} + \frac{2n\pi + \Delta n\pi}{2}\right) dx$$

Part 1:

$$\frac{1}{L}\int_{-\frac{L}{2}}^{\frac{L}{2}} xcos\left(-\frac{\Delta n\pi x}{L} - \frac{\Delta n\pi}{2}\right) dx$$

$$u = x \qquad dv = cos\left(-\frac{\Delta n\pi x}{L} - \frac{\Delta n\pi}{2}\right)$$

$$du = dx \qquad v = -\frac{L}{\Delta n\pi} sin\left(-\frac{\Delta n\pi x}{L} - \frac{\Delta n\pi}{2}\right) dx$$

$$-\frac{xL}{\Delta n\pi} sin\left(-\frac{\Delta n\pi x}{L} - \frac{\Delta n\pi}{2}\right) - \int -\frac{L}{\Delta n\pi} sin\left(-\frac{\Delta n\pi x}{L} - \frac{\Delta n\pi}{2}\right) dx$$

$$\frac{1}{L}\left(-\frac{Lx}{\Delta n\pi} sin\left(-\frac{\Delta n\pi x}{L} - \frac{\Delta n\pi}{2}\right) + \frac{L^2}{\Delta n^2\pi^2} cos\left(-\frac{\Delta n\pi x}{L} - \frac{\Delta n\pi}{2}\right)\right)\Bigg|_{\frac{-L}{2}}^{\frac{L}{2}} = -\frac{2L}{\Delta n^2\pi^2}$$

Part 2:

$$-\frac{1}{L}\int_{-\frac{L}{2}}^{\frac{L}{2}} x\cos\left(\frac{2n\pi x+\Delta n\pi x}{L}+\frac{2n\pi+\Delta n\pi}{2}\right)dx$$

$$u=x \qquad dv=\cos\left(\frac{2n\pi x+\Delta n\pi x}{L}+\frac{2n\pi+\Delta n\pi}{2}\right)dx$$

$$du=dx \qquad v=\frac{L}{2n\pi+\Delta n\pi}\sin\left(\frac{2n\pi x+\Delta n\pi x}{L}+\frac{2n\pi+\Delta n\pi}{2}\right)$$

$$\frac{xL}{2n\pi+\Delta n\pi}\sin\left(\frac{2n\pi x+\Delta n\pi x}{L}+\frac{2n\pi+\Delta n\pi}{2}\right)-\int\frac{L}{2n\pi+\Delta n\pi}\sin\left(\frac{2n\pi x+\Delta n\pi x}{L}+\frac{2n\pi+\Delta n\pi}{2}\right)dx$$

$$-\frac{1}{L}\left(\frac{xL}{2n\pi+\Delta n\pi}\sin\left(\frac{2n\pi+\Delta n\pi x}{L}+\frac{2n\pi+\Delta n\pi}{2}\right)+\frac{L^2}{(2n\pi+\Delta n\pi)^2}\cos\left(\frac{2n\pi x+\Delta n\pi x}{L}+\frac{2n\pi+\Delta n\pi}{2}\right)\right)\Bigg|_{\frac{-L}{2}}^{\frac{L}{2}}=\frac{2L}{(2n\pi+\Delta n\pi)^2}$$

$$-\frac{2L}{\Delta n^2\pi^2}+\frac{2L}{(2n\pi+\Delta n\pi)^2}$$

Transition Dipole Moment Integral for Particle in a box with an even Δn

$$\langle\psi_n|x|\psi_{n+\Delta n}\rangle$$

$$\int_{-\frac{L}{2}}^{\frac{L}{2}} x\sin\left(\frac{n\pi x}{L}+\frac{n\pi}{2}\right)\sin\left(\frac{(n+\Delta n)\pi x}{L}+\frac{(n+\Delta n)\pi}{2}\right)dx$$

$$\int_{-\frac{L}{2}}^{\frac{L}{2}} x\sin\left(\frac{n\pi x}{L}+\frac{n\pi}{2}\right)\sin\left(\frac{n\pi x}{L}+\frac{\Delta n\pi x}{L}+\frac{n\pi}{2}+\frac{\Delta n\pi}{2}\right)dx$$

$$\frac{2}{L}\int_{-\frac{L}{2}}^{\frac{L}{2}}\frac{x}{2}\left(\cos\left(\frac{n\pi x}{L}+\frac{n\pi}{2}-\frac{n\pi x+\Delta n\pi x}{L}-\frac{n\pi+\Delta n\pi}{2}\right)-\cos\left(\frac{n\pi x}{L}+\frac{n\pi}{2}+\frac{n\pi x+\Delta n\pi x}{L}+\frac{n\pi+\Delta n\pi}{2}\right)\right)dx$$

$$\frac{2}{L}\int_{-\frac{L}{2}}^{\frac{L}{2}}\frac{x}{2}\left(\cos\left(-\frac{\Delta n\pi x}{L}-\frac{\Delta n\pi}{2}\right)-\cos\left(\frac{2n\pi x+\Delta n\pi x}{L}+\frac{2n\pi+\Delta n\pi}{2}\right)\right)dx$$

$$\frac{1}{L}\int_{-\frac{L}{2}}^{\frac{L}{2}} x\cos\left(-\frac{\Delta n\pi x}{L}-\frac{\Delta n\pi}{2}\right)dx-\frac{1}{L}\int_{-\frac{L}{2}}^{\frac{L}{2}} x\cos\left(\frac{2n\pi x+\Delta n\pi x}{L}+\frac{2n\pi+\Delta n\pi}{2}\right)dx$$

Part 1:

$$\frac{1}{L}\int_{-\frac{L}{2}}^{\frac{L}{2}} x\cos\left(-\frac{\Delta n\pi x}{L}-\frac{\Delta n\pi}{2}\right)dx$$

$$u = x \qquad dv = \cos\left(-\frac{\Delta n\pi x}{L}-\frac{\Delta n\pi}{2}\right)$$

$$du = dx \qquad v = -\frac{L}{\Delta n\pi}\sin\left(-\frac{\Delta n\pi x}{L}-\frac{\Delta n\pi}{2}\right)dx$$

$$-\frac{xL}{\Delta n\pi}\sin\left(-\frac{\Delta n\pi x}{L}-\frac{\Delta n\pi}{2}\right)-\int -\frac{L}{\Delta n\pi}\sin\left(-\frac{\Delta n\pi x}{L}-\frac{\Delta n\pi}{2}\right)dx$$

$$\frac{1}{L}\left(-\frac{Lx}{\Delta n\pi}\sin\left(-\frac{\Delta n\pi x}{L}-\frac{\Delta n\pi}{2}\right)+\frac{L^2}{\Delta n^2\pi^2}\cos\left(-\frac{\Delta n\pi x}{L}-\frac{\Delta n\pi}{2}\right)\right)$$

$$\frac{1}{L}\left(-\frac{Lx}{\Delta n\pi}\sin\left(-\frac{\Delta n\pi x}{L}-\frac{\Delta n\pi}{2}\right)+\frac{L^2}{\Delta n^2\pi^2}\cos\left(-\frac{\Delta n\pi x}{L}-\frac{\Delta n\pi}{2}\right)\right)\Bigg|_{\frac{-L}{2}}^{\frac{L}{2}} = 0$$

Part 2:

$$-\frac{1}{L}\int_{-\frac{L}{2}}^{\frac{L}{2}} x\cos\left(\frac{2n\pi x+\Delta n\pi x}{L}+\frac{2n\pi+\Delta n\pi}{2}\right)dx$$

$$u = x \qquad dv = \cos\left(\frac{2n\pi x+\Delta n\pi x}{L}+\frac{2n\pi+\Delta n\pi}{2}\right)dx$$

$$du = dx \qquad v = \frac{L}{2n\pi+\Delta n\pi}\sin\left(\frac{2n\pi x+\Delta n\pi x}{L}+\frac{2n\pi+\Delta n\pi}{2}\right)$$

$$\frac{xL}{2n\pi+\Delta n\pi}\sin\left(\frac{2n\pi x+\Delta n\pi x}{L}+\frac{2n\pi+\Delta n\pi}{2}\right)-\int \frac{L}{2n\pi+\Delta n\pi}\sin\left(\frac{2n\pi x+\Delta n\pi x}{L}+\frac{2n\pi+\Delta n\pi}{2}\right)dx$$

$$-\frac{1}{L}\left(\frac{xL}{2n\pi+\Delta n\pi}\sin\left(\frac{2n\pi+\Delta n\pi x}{L}+\frac{2n\pi+\Delta n\pi}{2}\right)+\frac{L^2}{(2n\pi+\Delta n\pi)^2}\cos\left(\frac{2n\pi x+\Delta n\pi x}{L}+\frac{2n\pi+\Delta n\pi}{2}\right)\right)\Bigg|_{\frac{-L}{2}}^{\frac{L}{2}} = 0$$

Transition Dipole Moment Integral for Particle on a ring for an even or odd Δm_ℓ

$$\langle\psi_{m_\ell}|\cos\phi\,|\psi_{m_\ell+\Delta m_\ell}\rangle$$

$$\int_{-\pi}^{\pi} \sqrt{\frac{1}{2\pi}} e^{-im_\ell \phi} \cos\phi \sqrt{\frac{1}{2\pi}} e^{i(m_\ell + \Delta m_\ell)\phi} d\phi$$

$$\frac{1}{2\pi} \int_{-\pi}^{\pi} e^{i(-m_\ell + m_\ell + \Delta m_\ell)\phi} \cos\phi \, d\phi$$

$$\frac{1}{2\pi} \int_{-\pi}^{\pi} e^{i\Delta m_\ell \phi} \cos\phi \, d\phi$$

$$\frac{1}{2\pi} \int_{-\pi}^{\pi} (\cos(\Delta m_\ell \phi) + i \sin(\Delta m_\ell \phi)) \cos\phi \, d\phi$$

$$\frac{1}{2\pi} \int_{-\pi}^{\pi} \cos(\Delta m_\ell \phi) \cos\phi + i \sin(\Delta m_\ell \phi) \cos\phi \, d\phi$$

$$\frac{1}{2\pi} \int_{-\pi}^{\pi} \cos(\Delta m_\ell \phi) \cos\phi \, d\phi + \frac{1}{2\pi} \int_{-\pi}^{\pi} i \sin(\Delta m_\ell \phi) \cos\phi \, d\phi$$

Part 1:

$$\frac{1}{2\pi} \int_{-\pi}^{\pi} \frac{1}{2} [\cos(\Delta m_\ell \phi - \phi) + \cos(\Delta m_\ell \phi + \phi)] \, d\phi$$

$$\frac{1}{4\pi} \int_{-\pi}^{\pi} \cos(\Delta m_\ell \phi - \phi) d\phi + \frac{1}{4\pi} \int_{-\pi}^{\pi} \cos(\Delta m_\ell \phi + \phi) d\phi$$

$$\frac{1}{4\pi(\Delta m_\ell - 1)} \sin(\Delta m_\ell \phi - \phi) + \frac{1}{4\pi(\Delta m_\ell + 1)} \sin(\Delta m_\ell \phi + \phi) \Big|_{-\pi}^{\pi} = 0$$

Part 2:

$$\frac{i}{2\pi} \int_{-\pi}^{\pi} \frac{1}{2} [\sin(\Delta m_\ell \phi + \phi) + \sin(\Delta m_\ell \phi - \phi)] \, d\phi$$

$$\frac{i}{4\pi} \int_{-\pi}^{\pi} \sin(\Delta m_\ell \phi + \phi) \, d\phi + \frac{i}{4\pi} \int_{-\pi}^{\pi} \sin(\Delta m_\ell \phi - \phi) \, d\phi$$

$$-\frac{i}{4\pi(\Delta m_\ell + 1)} \cos(\Delta m_\ell \phi + \phi) - \frac{i}{4\pi(\Delta m_\ell - 1)} \cos(\Delta m_\ell \phi - \phi) \Big|_{-\pi}^{\pi} = 0$$

Transition Dipole Moment Integral for Particle on a ring for a $\Delta m_\ell = 1$

$$\langle \psi_{m_\ell} | \cos\phi \, | \psi_{m_\ell+1} \rangle$$

$$\int_{-\pi}^{\pi} \sqrt{\frac{1}{2\pi}} e^{-im_\ell\phi} \cos\phi \sqrt{\frac{1}{2\pi}} e^{i(m_\ell+1)\phi} d\phi$$

$$\frac{1}{2\pi} \int_{-\pi}^{\pi} e^{i(-m_\ell+m_\ell+1)\phi} \cos\phi \, d\phi$$

$$\frac{1}{2\pi} \int_{-\pi}^{\pi} e^{i\phi} \cos\phi \, d\phi$$

$$\frac{1}{2\pi} \int_{-\pi}^{\pi} (\cos\phi + i\sin\phi) \cos\phi \, d\phi$$

$$\frac{1}{2\pi} \int_{-\pi}^{\pi} \cos(\phi)\cos\phi + i\sin(\phi)\cos\phi \, d\phi$$

$$\frac{1}{2\pi} \int_{-\pi}^{\pi} \cos\phi\cos\phi \, d\phi + \frac{1}{2\pi} \int_{-\pi}^{\pi} i\sin\phi\cos\phi \, d\phi$$

Part 1:

$$\frac{1}{2\pi} \int_{-\pi}^{\pi} \cos^2\phi \, d\phi$$

$$\frac{1}{2\pi} \int_{-\pi}^{\pi} \frac{1}{2}(1-\cos\phi) d\phi$$

$$\frac{1}{4\pi} \int_{-\pi}^{\pi} 1 - \cos\phi \, d\phi$$

$$\frac{1}{4\pi} \int_{-\pi}^{\pi} d\phi - \frac{1}{4\pi} \int_{-\pi}^{\pi} \cos\phi \, d\phi$$

$$\frac{\phi}{4\pi} - \frac{1}{4\pi} \sin\phi \Big|_{-\pi}^{\pi} = \frac{1}{2}$$

Part 2:

$$\frac{1}{2\pi}\int_{-\pi}^{\pi} i \sin\phi \cos\phi \, d\phi$$

$$\frac{i}{2\pi}\int_{-\pi}^{\pi} \frac{1}{2}[\sin(\Delta m_\ell \phi + \phi) + \sin(\Delta m_\ell \phi - \phi)] \, d\phi$$

$$\frac{i}{4\pi}\int_{-\pi}^{\pi} \sin(\Delta m_\ell \phi + \phi) \, d\phi + \frac{i}{4\pi}\int_{-\pi}^{\pi} \sin(\Delta m_\ell \phi - \phi) \, d\phi$$

$$-\frac{i}{4\pi(\Delta m_\ell + 1)}\cos(\Delta m_\ell \phi + \phi) - \frac{i}{4\pi(\Delta m_\ell - 1)}\cos(\Delta m_\ell \phi - \phi)\Big|_{-\pi}^{\pi} = 0$$

APPENDIX E

Transition Moment Integral for Particle in a Box for an odd Δn

$$\langle\psi_n|x^2|\psi_{n+\Delta n}\rangle$$

$$\int_{-\frac{L}{2}}^{\frac{L}{2}} x^2 \sqrt{\frac{2}{L}} sin\left(\frac{n\pi x}{L}+\frac{n\pi}{2}\right)\sqrt{\frac{2}{L}} sin\left(\frac{(n+\Delta n)\pi x}{L}+\frac{(n+\Delta n)\pi}{2}\right)dx$$

$$\frac{2}{L}\int_{-\frac{L}{2}}^{\frac{L}{2}} x^2 sin\left(\frac{n\pi x}{L}+\frac{n\pi}{2}\right) sin\left(\frac{n\pi x}{L}+\frac{\Delta n\pi x}{L}+\frac{n\pi}{2}+\frac{\Delta n\pi}{2}\right)dx$$

$$\frac{2}{L}\int_{-\frac{L}{2}}^{\frac{L}{2}} \frac{x^2}{2}\left[cos\left(\frac{n\pi x}{L}+\frac{\Delta n\pi x}{L}+\frac{n\pi}{2}+\frac{\Delta n\pi}{2}-\frac{n\pi x}{L}-\frac{n\pi}{2}\right)-cos\left(\frac{n\pi x}{L}+\frac{\Delta n\pi x}{L}+\frac{n\pi}{2}+\frac{\Delta n\pi}{2}+\frac{n\pi x}{L}+\frac{n\pi}{2}\right)\right]dx$$

$$\frac{1}{L}\int_{-\frac{L}{2}}^{\frac{L}{2}} x^2\left[cos\left(\frac{\Delta n\pi x}{L}+\frac{\Delta n\pi}{2}\right)-cos\left(\frac{2n\pi x}{L}+n\pi+\frac{\Delta n\pi x}{L}+\frac{\Delta n\pi}{2}\right)\right]dx$$

$$\frac{1}{L}\int_{-\frac{L}{2}}^{\frac{L}{2}} x^2 cos\left(\frac{\Delta n\pi x}{L}+\frac{\Delta n\pi}{2}\right)dx-\frac{1}{L}\int_{-\frac{L}{2}}^{\frac{L}{2}} x^2 cos\left(\frac{2n\pi x}{L}+n\pi+\frac{\Delta n\pi x}{L}+\frac{\Delta n\pi}{2}\right)dx$$

Part 1:

$$\frac{1}{L}\int_{-\frac{L}{2}}^{\frac{L}{2}} x^2 cos\left(\frac{\Delta n\pi x}{L}+\frac{\Delta n\pi}{2}\right)dx$$

$$u=x^2 \quad dv=cos\left(\frac{\Delta n\pi x}{L}+\frac{\Delta n\pi}{2}\right)dx$$

$$du=2xdx \;\; v=\frac{L}{\Delta n\pi}\sin\left(\frac{\Delta n\pi x}{L}+\frac{\Delta n\pi}{2}\right)$$

$$\frac{Lx^2}{\Delta n\pi}\sin\left(\frac{\Delta n\pi x}{L}+\frac{\Delta n\pi}{2}\right)-\int\frac{2Lx}{\Delta n\pi}\sin\left(\frac{\Delta n\pi x}{L}+\frac{\Delta n\pi}{2}\right)dx$$

$$u=\frac{2Lx}{\Delta n\pi} \quad dv=\sin\left(\frac{\Delta n\pi x}{L}+\frac{\Delta n\pi}{2}\right)dx$$

$$du=\frac{2L}{\Delta n\pi}dx \quad v=-\frac{L}{\Delta n\pi}\cos\left(\frac{\Delta n\pi x}{L}+\frac{\Delta n\pi}{2}\right)$$

$$-\frac{2L^2x}{\Delta n^2\pi^2}\cos\left(\frac{\Delta n\pi x}{L}+\frac{\Delta n\pi}{2}\right)+\int\frac{2L^2}{\Delta n^2\pi^2}\cos\left(\frac{\Delta n\pi x}{L}+\frac{\Delta n\pi}{2}\right)dx$$

$$-\frac{2L^2x}{\Delta n^2\pi^2}\cos\left(\frac{\Delta n\pi x}{L}+\frac{\Delta n\pi}{2}\right)+\frac{2L^3}{\Delta n^3\pi^3}\sin\left(\frac{\Delta n\pi x}{L}+\frac{\Delta n\pi}{2}\right)$$

$$\frac{1}{L}\left[\frac{Lx^2}{\Delta n\pi}\sin\left(\frac{\Delta n\pi x}{L}+\frac{\Delta n\pi}{2}\right)+\frac{2L^2x}{\Delta n^2\pi^2}\cos\left(\frac{\Delta n\pi x}{L}+\frac{\Delta n\pi}{2}\right)-\frac{2L^3}{\Delta n^3\pi^3}\sin\left(\frac{\Delta n\pi x}{L}+\frac{\Delta n\pi}{2}\right)\right]$$

$$\frac{x^2}{\Delta n\pi}\sin\left(\frac{\Delta n\pi x}{L}+\frac{\Delta n\pi}{2}\right)+\frac{2Lx}{\Delta n^2\pi^2}\cos\left(\frac{\Delta n\pi x}{L}+\frac{\Delta n\pi}{2}\right)-\frac{2L^2}{\Delta n^3\pi^3}\sin\left(\frac{\Delta n\pi x}{L}+\frac{\Delta n\pi}{2}\right)\Bigg|_{\frac{-L}{2}}^{\frac{L}{2}}=0$$

Part 2:

$$-\frac{1}{L}\int_{-\frac{L}{2}}^{\frac{L}{2}}x^2cos\left(\frac{2n\pi x}{L}+n\pi+\frac{\Delta n\pi x}{L}+\frac{\Delta n\pi}{2}\right)dx$$

$$u=x^2\quad dv=cos\left(\frac{2n\pi x}{L}+n\pi+\frac{\Delta n\pi x}{L}+\frac{\Delta n\pi}{2}\right)dx$$

$$du=2xdx\quad v=\frac{L}{2n\pi+\Delta n\pi}\sin\left(\frac{2n\pi x}{L}+n\pi+\frac{\Delta n\pi x}{L}+\frac{\Delta n\pi}{2}\right)$$

$$\frac{Lx^2}{2n\pi+\Delta n\pi}\sin\left(\frac{2n\pi x}{L}+n\pi+\frac{\Delta n\pi x}{L}+\frac{\Delta n\pi}{2}\right)-\int\frac{2Lx}{2n\pi+\Delta n\pi}\sin\left(\frac{2n\pi x}{L}+n\pi+\frac{\Delta n\pi x}{L}+\frac{\Delta n\pi}{2}\right)dx$$

$$u=\frac{2Lx}{2n\pi+\Delta n\pi}\qquad dv=\sin\left(\frac{2n\pi x}{L}+n\pi+\frac{\Delta n\pi x}{L}+\frac{\Delta n\pi}{2}\right)dx$$

$$du=\frac{2L}{2n\pi+\Delta n\pi}dx\quad v=-\frac{L}{2n\pi+\Delta n\pi}\cos\left(\frac{2n\pi x}{L}+n\pi+\frac{\Delta n\pi x}{L}+\frac{\Delta n\pi}{2}\right)$$

$$-\frac{2L^2x}{(2n\pi+\Delta n\pi)^2}\cos\left(\frac{2n\pi x}{L}+n\pi+\frac{\Delta n\pi x}{L}+\frac{\Delta n\pi}{2}\right)+\int\frac{2L^2}{(2n\pi+\Delta n\pi)^2}\cos\left(\frac{2n\pi x}{L}+n\pi+\frac{\Delta n\pi x}{L}+\frac{\Delta n\pi}{2}\right)dx$$

$$-\frac{2L^2x}{(2n\pi+\Delta n\pi)^2}\cos\left(\frac{2n\pi x}{L}+n\pi+\frac{\Delta n\pi x}{L}+\frac{\Delta n\pi}{2}\right)+\frac{2L^3}{(2n\pi+\Delta n\pi)^3}\sin\left(\frac{2n\pi x}{L}+n\pi+\frac{\Delta n\pi x}{L}+\frac{\Delta n\pi}{2}\right)$$

$$-\frac{1}{L}\left[\frac{Lx^2}{2n\pi+\Delta n\pi}\sin\left(\frac{2n\pi x}{L}+n\pi+\frac{\Delta n\pi x}{L}+\frac{\Delta n\pi}{2}\right)+\frac{2L^2x}{(2n\pi+\Delta n\pi)^2}\cos\left(\frac{2n\pi x}{L}+n\pi+\frac{\Delta n\pi x}{L}+\frac{\Delta n\pi}{2}\right)-\frac{2L^3}{(2n\pi+\Delta n\pi)^3}\sin\left(\frac{2n\pi x}{L}+n\pi+\frac{\Delta n\pi x}{L}+\frac{\Delta n\pi}{2}\right)\right]$$

$$-\frac{x^2}{2n\pi+\Delta n\pi}\sin\left(\frac{2n\pi x}{L}+n\pi+\frac{\Delta n\pi x}{L}+\frac{\Delta n\pi}{2}\right)-\frac{2Lx}{(2n\pi+\Delta n\pi)^2}\cos\left(\frac{2n\pi x}{L}+n\pi+\frac{\Delta n\pi x}{L}+\frac{\Delta n\pi}{2}\right)+\frac{2L^2}{(2n\pi+\Delta n\pi)^3}\sin\left(\frac{2n\pi x}{L}+n\pi+\frac{\Delta n\pi x}{L}+\frac{\Delta n\pi}{2}\right)\Bigg|_{\frac{-L}{2}}^{\frac{L}{2}}=0$$

Transition Moment Integral for Particle in a Box for an even Δn

$$\langle \psi_n | x^2 | \psi_{n+\Delta n} \rangle$$

$$\int_{-\frac{L}{2}}^{\frac{L}{2}} x^2 \sqrt{\frac{2}{L}} sin\left(\frac{n\pi x}{L} + \frac{n\pi}{2}\right) \sqrt{\frac{2}{L}} sin\left(\frac{(n+\Delta n)\pi x}{L} + \frac{(n+\Delta n)\pi}{2}\right) dx$$

$$\frac{2}{L}\int_{-\frac{L}{2}}^{\frac{L}{2}} x^2 sin\left(\frac{n\pi x}{L} + \frac{n\pi}{2}\right) sin\left(\frac{n\pi x}{L} + \frac{\Delta n\pi x}{L} + \frac{n\pi}{2} + \frac{\Delta n\pi}{2}\right) dx$$

$$\frac{2}{L}\int_{-\frac{L}{2}}^{\frac{L}{2}} \frac{x^2}{2}\left[cos\left(\frac{n\pi x}{L} + \frac{\Delta n\pi x}{L} + \frac{n\pi}{2} + \frac{\Delta n\pi}{2} - \frac{n\pi x}{L} - \frac{n\pi}{2}\right) - cos\left(\frac{n\pi x}{L} + \frac{\Delta n\pi x}{L} + \frac{n\pi}{2} + \frac{\Delta n\pi}{2} + \frac{n\pi x}{L} + \frac{n\pi}{2}\right)\right] dx$$

$$\frac{1}{L}\int_{-\frac{L}{2}}^{\frac{L}{2}} x^2 \left[cos\left(\frac{\Delta n\pi x}{L} + \frac{\Delta n\pi}{2}\right) - cos\left(\frac{2n\pi x}{L} + n\pi + \frac{\Delta n\pi x}{L} + \frac{\Delta n\pi}{2}\right)\right] dx$$

$$\frac{1}{L}\int_{-\frac{L}{2}}^{\frac{L}{2}} x^2 cos\left(\frac{\Delta n\pi x}{L} + \frac{\Delta n\pi}{2}\right) dx - \frac{1}{L}\int_{-\frac{L}{2}}^{\frac{L}{2}} x^2 cos\left(\frac{2n\pi x}{L} + n\pi + \frac{\Delta n\pi x}{L} + \frac{\Delta n\pi}{2}\right) dx$$

Part 1:

$$\frac{1}{L}\int_{-\frac{L}{2}}^{\frac{L}{2}} x^2 cos\left(\frac{\Delta n\pi x}{L} + \frac{\Delta n\pi}{2}\right) dx$$

$$u = x^2 \quad dv = cos\left(\frac{\Delta n\pi x}{L} + \frac{\Delta n\pi}{2}\right) dx$$

$$du = 2xdx \;\; v = \frac{L}{\Delta n\pi}\sin\left(\frac{\Delta n\pi x}{L} + \frac{\Delta n\pi}{2}\right)$$

$$\frac{Lx^2}{\Delta n\pi}\sin\left(\frac{\Delta n\pi x}{L} + \frac{\Delta n\pi}{2}\right) - \int \frac{2Lx}{\Delta n\pi}\sin\left(\frac{\Delta n\pi x}{L} + \frac{\Delta n\pi}{2}\right) dx$$

$$u = \frac{2Lx}{\Delta n\pi} \quad dv = \sin\left(\frac{\Delta n\pi x}{L} + \frac{\Delta n\pi}{2}\right) dx$$

$$du = \frac{2L}{\Delta n\pi} dx \quad v = -\frac{L}{\Delta n\pi}\cos\left(\frac{\Delta n\pi x}{L} + \frac{\Delta n\pi}{2}\right)$$

$$-\frac{2L^2x}{\Delta n^2\pi^2}\cos\left(\frac{\Delta n\pi x}{L}+\frac{\Delta n\pi}{2}\right)+\int\frac{2L^2}{\Delta n^2\pi^2}\cos\left(\frac{\Delta n\pi x}{L}+\frac{\Delta n\pi}{2}\right)dx$$

$$-\frac{2L^2x}{\Delta n^2\pi^2}\cos\left(\frac{\Delta n\pi x}{L}+\frac{\Delta n\pi}{2}\right)+\frac{2L^3}{\Delta n^3\pi^3}\sin\left(\frac{\Delta n\pi x}{L}+\frac{\Delta n\pi}{2}\right)$$

$$\frac{1}{L}\left[\frac{Lx^2}{\Delta n\pi}\sin\left(\frac{\Delta n\pi x}{L}+\frac{\Delta n\pi}{2}\right)+\frac{2L^2x}{\Delta n^2\pi^2}\cos\left(\frac{\Delta n\pi x}{L}+\frac{\Delta n\pi}{2}\right)-\frac{2L^3}{\Delta n^3\pi^3}\sin\left(\frac{\Delta n\pi x}{L}+\frac{\Delta n\pi}{2}\right)\right]$$

$$\frac{x^2}{\Delta n\pi}\sin\left(\frac{\Delta n\pi x}{L}+\frac{\Delta n\pi}{2}\right)+\frac{2Lx}{\Delta n^2\pi^2}\cos\left(\frac{\Delta n\pi x}{L}+\frac{\Delta n\pi}{2}\right)-\frac{2L^2}{\Delta n^3\pi^3}\sin\left(\frac{\Delta n\pi x}{L}+\frac{\Delta n\pi}{2}\right)\Bigg|_{\frac{-L}{2}}^{\frac{L}{2}}=\frac{2L^2}{\Delta n\pi}$$

Part 2:

$$-\frac{1}{L}\int_{-\frac{L}{2}}^{\frac{L}{2}}x^2cos\left(\frac{2n\pi x}{L}+n\pi+\frac{\Delta n\pi x}{L}+\frac{\Delta n\pi}{2}\right)dx$$

$$u=x^2\quad dv=cos\left(\frac{2n\pi x}{L}+n\pi+\frac{\Delta n\pi x}{L}+\frac{\Delta n\pi}{2}\right)dx$$

$$du=2xdx\quad v=\frac{L}{2n\pi+\Delta n\pi}\sin\left(\frac{2n\pi x}{L}+n\pi+\frac{\Delta n\pi x}{L}+\frac{\Delta n\pi}{2}\right)$$

$$\frac{Lx^2}{2n\pi+\Delta n\pi}\sin\left(\frac{2n\pi x}{L}+n\pi+\frac{\Delta n\pi x}{L}+\frac{\Delta n\pi}{2}\right)-\int\frac{2Lx}{2n\pi+\Delta n\pi}\sin\left(\frac{2n\pi x}{L}+n\pi+\frac{\Delta n\pi x}{L}+\frac{\Delta n\pi}{2}\right)dx$$

$$u=\frac{2Lx}{2n\pi+\Delta n\pi}\qquad dv=\sin\left(\frac{2n\pi x}{L}+n\pi+\frac{\Delta n\pi x}{L}+\frac{\Delta n\pi}{2}\right)dx$$

$$du=\frac{2L}{2n\pi+\Delta n\pi}dx\quad v=-\frac{L}{2n\pi+\Delta n\pi}\cos\left(\frac{2n\pi x}{L}+n\pi+\frac{\Delta n\pi x}{L}+\frac{\Delta n\pi}{2}\right)$$

$$-\frac{2L^2x}{(2n\pi+\Delta n\pi)^2}\cos\left(\frac{2n\pi x}{L}+n\pi+\frac{\Delta n\pi x}{L}+\frac{\Delta n\pi}{2}\right)+\int\frac{2L^2}{(2n\pi+\Delta n\pi)^2}\cos\left(\frac{2n\pi x}{L}+n\pi+\frac{\Delta n\pi x}{L}+\frac{\Delta n\pi}{2}\right)dx$$

$$-\frac{2L^2x}{(2n\pi+\Delta n\pi)^2}\cos\left(\frac{2n\pi x}{L}+n\pi+\frac{\Delta n\pi x}{L}+\frac{\Delta n\pi}{2}\right)+\frac{2L^3}{(2n\pi+\Delta n\pi)^3}\sin\left(\frac{2n\pi x}{L}+n\pi+\frac{\Delta n\pi x}{L}+\frac{\Delta n\pi}{2}\right)$$

$$-\frac{1}{L}\left[\frac{Lx^2}{2n\pi+\Delta n\pi}\sin\left(\frac{2n\pi x}{L}+n\pi+\frac{\Delta n\pi x}{L}+\frac{\Delta n\pi}{2}\right)+\frac{2L^2x}{(2n\pi+\Delta n\pi)^2}\cos\left(\frac{2n\pi x}{L}+n\pi+\frac{\Delta n\pi x}{L}+\frac{\Delta n\pi}{2}\right)-\frac{2L^3}{(2n\pi+\Delta n\pi)^3}\sin\left(\frac{2n\pi x}{L}+n\pi+\frac{\Delta n\pi x}{L}+\frac{\Delta n\pi}{2}\right)\right]$$

$$-\frac{x^2}{2n\pi+\Delta n\pi}\sin\left(\frac{2n\pi x}{L}+n\pi+\frac{\Delta n\pi x}{L}+\frac{\Delta n\pi}{2}\right)-\frac{2Lx}{(2n\pi+\Delta n\pi)^2}\cos\left(\frac{2n\pi x}{L}+n\pi+\frac{\Delta n\pi x}{L}+\frac{\Delta n\pi}{2}\right)+\frac{2L^2}{(2n\pi+\Delta n\pi)^3}\sin\left(\frac{2n\pi x}{L}+n\pi+\frac{\Delta n\pi x}{L}+\frac{\Delta n\pi}{2}\right)\Bigg|_{\frac{-L}{2}}^{\frac{L}{2}}=-\frac{2L^2}{(2n\pi+\Delta n\pi)^2}$$

$$\frac{2L^2}{\Delta n\pi} - \frac{2L^2}{(2n\pi + \Delta n\pi)^2}$$

Transition Moment Integral for Particle on a ring for odd and even Δm_ℓ

$$\langle \psi_{m_\ell} | \cos^2 \phi \, | \psi_{m_\ell + \Delta m_\ell} \rangle$$

$$\int_{-\pi}^{\pi} \sqrt{\frac{1}{2\pi}} e^{-im_\ell \phi} \cos^2 \phi \sqrt{\frac{1}{2\pi}} e^{i(m_\ell + \Delta m_\ell)\phi} d\phi$$

$$\frac{1}{2\pi} \int_{-\pi}^{\pi} e^{i(-m_\ell + m_\ell + \Delta m_\ell)\phi} \cos^2 \phi \, d\phi$$

$$\frac{1}{2\pi} \int_{-\pi}^{\pi} \frac{1}{2} e^{i(\Delta m_\ell)\phi} d\phi + \frac{1}{2\pi} \int_{-\pi}^{\pi} \frac{1}{2} \cos(2\phi) \, e^{i(\Delta m_\ell)\phi} d\phi$$

$$\frac{1}{4\pi} \int_{-\pi}^{\pi} e^{i(\Delta m_\ell)\phi} d\phi + \frac{1}{4\pi} \int_{-\pi}^{\pi} \cos(2\phi) \, e^{i(\Delta m_\ell)\phi} d\phi$$

$$\frac{1}{4\pi} \int_{-\pi}^{\pi} e^{i(\Delta m_\ell)\phi} d\phi + \frac{1}{4\pi} \int_{-\pi}^{\pi} \cos(2\phi)[\cos(\Delta m_\ell \phi) + i \sin(\Delta m_\ell \phi)] \, d\phi$$

$$\frac{1}{4\pi} \int_{-\pi}^{\pi} e^{i(\Delta m_\ell)\phi} d\phi + \frac{1}{4\pi} \int_{-\pi}^{\pi} \cos(\Delta m_\ell \phi) \cos(2\phi) + i \sin(\Delta m_\ell \phi) \cos(2\phi) \, d\phi$$

$$\frac{1}{4\pi} \int_{-\pi}^{\pi} e^{i(\Delta m_\ell)\phi} d\phi + \frac{1}{4\pi} \int_{-\pi}^{\pi} \cos(\Delta m_\ell \phi) \cos(2\phi) \, d\phi + \frac{1}{4\pi} \int_{-\pi}^{\pi} i \sin(\Delta m_\ell \phi) \cos(2\phi) \, d\phi$$

Part 1:

$$\frac{1}{4\pi} \int_{-\pi}^{\pi} e^{i2\phi} d\phi$$

$$\frac{1}{i8\pi} e^{i2\phi} \Big|_{-\pi}^{\pi} = 0$$

Part 2:

$$\frac{1}{4\pi} \int_{-\pi}^{\pi} \cos(\Delta m_\ell \phi) \cos(2\phi) \, d\phi$$

$$\frac{1}{4\pi}\int_{-\pi}^{\pi}\frac{1}{2}[\cos(\Delta m_\ell\phi-2\phi)+\cos(\Delta m_\ell\phi+2\phi)]d\phi$$

$$\frac{1}{8\pi}\int_{-\pi}^{\pi}\cos(\Delta m_\ell\phi-2\phi)\,d\phi+\frac{1}{8\pi}\int_{-\pi}^{\pi}\cos(\Delta m_\ell\phi+2\phi)\,d\phi$$

$$\frac{1}{8\pi(\Delta m_\ell-2)}\sin(\Delta m_\ell\phi-2\phi)+\frac{1}{8\pi(\Delta m_\ell+2)}\sin(\Delta m_\ell\phi+2\phi)\Big|_{-\pi}^{\pi}=0$$

Part 3:

$$\frac{1}{4\pi}\int_{-\pi}^{\pi}i\sin(\Delta m_\ell\phi)\cos(2\phi)\,d\phi$$

$$\frac{i}{2\pi}\int_{-\pi}^{\pi}\frac{1}{2}[\sin(\Delta m_\ell\phi+2\phi)+\sin(\Delta m_\ell\phi-2\phi)]\,d\phi$$

$$\frac{i}{4\pi}\int_{-\pi}^{\pi}\sin(\Delta m_\ell\phi+2\phi)\,d\phi+\frac{i}{4\pi}\int_{-\pi}^{\pi}\sin(\Delta m_\ell\phi-2\phi)\,d\phi$$

$$-\frac{i}{4\pi(\Delta m_\ell+2)}\cos(\Delta m_\ell\phi+2\phi)-\frac{i}{4\pi(\Delta m_\ell-2)}\cos(\Delta m_\ell\phi-2\phi)\Big|_{-\pi}^{\pi}=0$$

Transition Moment Integral for Particle on a ring for $\Delta m_\ell=2$

$$\langle\psi_{m_\ell}|\cos^2\phi\,|\psi_{m_\ell+2}\rangle$$

$$\int_{-\pi}^{\pi}\sqrt{\frac{1}{2\pi}}e^{-im_\ell\phi}\cos^2\phi\sqrt{\frac{1}{2\pi}}e^{i(m_\ell+2)\phi}d\phi$$

$$\frac{1}{2\pi}\int_{-\pi}^{\pi}e^{i(-m_\ell+m_\ell+2)\phi}\cos^2\phi\,d\phi$$

$$\frac{1}{2\pi}\int_{-\pi}^{\pi}\frac{1}{2}e^{i2\phi}d\phi+\frac{1}{2\pi}\int_{-\pi}^{\pi}\frac{1}{2}\cos(2\phi)\,e^{i2\phi}d\phi$$

$$\frac{1}{4\pi}\int_{-\pi}^{\pi}e^{i2\phi}d\phi+\frac{1}{4\pi}\int_{-\pi}^{\pi}\cos(2\phi)\,e^{i2\phi}d\phi$$

$$\frac{1}{4\pi}\int_{-\pi}^{\pi} e^{i2\phi}d\phi + \frac{1}{4\pi}\int_{-\pi}^{\pi} \cos(2\phi)[\cos(2\phi) + i\sin(2\phi)]\,d\phi$$

$$\frac{1}{4\pi}\int_{-\pi}^{\pi} e^{i2\phi}d\phi + \frac{1}{4\pi}\int_{-\pi}^{\pi} \cos(2\phi)\cos(2\phi) + i\sin(2\phi)\cos(2\phi)\,d\phi$$

$$\frac{1}{4\pi}\int_{-\pi}^{\pi} e^{i2\phi}d\phi + \frac{1}{4\pi}\int_{-\pi}^{\pi} \cos(2\phi)\cos(2\phi)\,d\phi + \frac{1}{4\pi}\int_{-\pi}^{\pi} i\sin(2\phi)\cos(2\phi)\,d\phi$$

Part 1:

$$\frac{1}{4\pi}\int_{-\pi}^{\pi} e^{i2\phi}d\phi$$

$$\frac{1}{i8\pi}e^{i2\phi}\Big|_{-\pi}^{\pi} = 0$$

Part 2:

$$\frac{1}{4\pi}\int_{-\pi}^{\pi} \cos(2\phi)\cos(2\phi)\,d\phi$$

$$\frac{1}{4\pi}\int_{-\pi}^{\pi} \cos^2(2\phi)\,d\phi$$

$$\frac{1}{4\pi}\int_{-\pi}^{\pi} \frac{1}{2}[1 - \cos(4\phi)]d\phi$$

$$\frac{1}{8\pi}\int_{-\pi}^{\pi} d\phi - \frac{1}{8\pi}\int_{-\pi}^{\pi} \cos(4\phi)\,d\phi$$

$$\frac{\phi}{8\pi} - \frac{1}{32\pi}\sin(4\phi)\Big|_{-\pi}^{\pi} = \frac{1}{4}$$

Part 3:

$$\frac{1}{4\pi}\int_{-\pi}^{\pi} i\sin(2\phi)\cos(2\phi)\,d\phi$$

$$\frac{i}{4\pi}\int_{-\pi}^{\pi} \frac{1}{2}[\sin(2\phi + 2\phi) + \sin(2\phi - 2\phi)]\,d\phi$$

$$-\frac{i}{32\pi}\cos(4\phi)\Big|_{-\pi}^{\pi} = 0$$

Transition Moment Integral for Particle on a ring for $\Delta m_\ell = 0$

$$\langle \psi_{m_\ell} | \cos^2 \phi \, | \psi_{m_\ell} \rangle$$

$$\int_{-\pi}^{\pi} \sqrt{\frac{1}{2\pi}} e^{-i m_\ell \phi} \cos^2 \phi \sqrt{\frac{1}{2\pi}} e^{i m_\ell \phi} d\phi$$

$$\frac{1}{2\pi} \int_{-\pi}^{\pi} e^{i(-m_\ell + m_\ell)\phi} \cos^2 \phi \, d\phi$$

$$\frac{1}{2\pi} \int_{-\pi}^{\pi} \cos^2 \phi \, d\phi$$

$$\frac{1}{2\pi} \int_{-\pi}^{\pi} \frac{1}{2} [1 + \cos(2\phi)] d\phi$$

$$\frac{1}{2\pi} \int_{-\pi}^{\pi} \frac{1}{2} d\phi + \frac{1}{2\pi} \int_{-\pi}^{\pi} \frac{1}{2} \cos(2\phi) \, d\phi$$

$$\frac{\phi}{4\pi} + \frac{1}{8\pi} \sin(2\phi) \Big|_{-\pi}^{\pi} = \frac{1}{4}$$

VITA

Victoria A. Spenn

Education

Masters of Science student in Chemistry at Sam Houston State University, January 2014 – present. Thesis title “The Schrödinger equation to spectroscopy: a simplified quantum mechanical connection”.

Bachelor of Science (December 2013) in Chemistry, Sam Houston State University, Huntsville, Texas.

Bachelor of Science (May 2008) in Nutritional Science, Texas A&M University, College Station, Texas

Academic Employment

Graduate Teaching Assistant, Department of Chemistry, Sam Houston State University, August 2014-present. Responsibilities include: assisting professors with the preparation and presentation of undergraduate courses, grading, and tutoring.

Publications

Jackson, V.S., and D.L. Williams. (In review). Particle on a Ring Spectroscopic Selection Rules Determined by Group Theory. Journal of Chemical Education.